# Mini Review of Technological Trends of Flexible Supercapacitors Using Carbon Nanotubes

Haeji Kim, Jun Young Cheong & Byungil Hwang

Published online: 21 Apr 2023.

Submit your article to this journal ⍈

Article views: 264

View related articles ⍈

View Crossmark data ⍈

Taylor & Francis
Taylor & Francis Group

# Mini Review of Technological Trends of Flexible Supercapacitors Using Carbon Nanotubes

Haeji Kim[a], Jun Young Cheong[b], and Byungil Hwang[a]

[a]School of Integrative Engineering, Chung-Ang University, Seoul, Republic of Korea; [b]Bavarian Center for Battery Technology (BayBatt) and Department of Chemistry, University of Bayreuth, Bayreuth, Germany

## ABSTRACT

With the technological advances in wearable and portable electronic devices, the demands for associated technologies including flexible energy storage devices increase. Among many types of energy storage devices, flexible supercapacitors (FSCs) are highly attractive in comparison with others as they exhibit high power density, high storage density, and mechanical stability. In particular, carbon nanotubes (CNTs) are being widely used as the electrode materials for FSCs, owing to their mechanical strength and outstanding electrical performance. Herein, we classified CNT-based FSCs according to the structural types of CNTs and the materials incorporated. The unique structures and properties of the three types of CNTs (single-walled CNTs (SWCNT), double-walled CNTs (DWCNT), and multi-walled CNTs (MWCNT)) are compared and the mechanisms of FSCs are discussed. Finally, a summary of the overall electrochemical properties and current development of the reported FSC electrodes based on SWCNT, DWCNT, and MWCNT are presented thoroughly.

### 摘要

随着可穿戴和便携式电子设备的技术进步, 对包括柔性储能设备在内的相关技术的需求增加. 在许多类型的能量存储设备中, 柔性超级电容器(FSCs)与其他超级电容器相比极具吸引力, 因为它们表现出高功率密度、高存储密度和机械稳定性. 特别地, 碳纳米管(CNTs)由于其机械强度和优异的电性能而被广泛用作FSC的电极材料. 在此, 我们根据CNT的结构类型和所掺入的材料对基于CNT的FSCs进行了分类. 比较了三种CNT(单壁CNT(SWCNT)、双壁CNT和多壁CNT)的独特结构和财产, 并讨论了FSC的机理. 最后, 对基于SWCNT、DWCNT和MWCNT的FSC电极的整体电化学财产和当前发展进行了全面总结.

## Introduction

Stretchable and flexible electronic devices are considered highly attractive due to the emergence of portable electronic devices (Kim and Rogers 2008; Lim et al. 2020). In particular, with the current issues regarding energy supply, the development of flexible energy storage devices is becoming a necessity (Chen et al. 2020; Gong et al. 2021; Vangari, Pryor, and Jiang 2013). Among the types of energy storage devices, flexible supercapacitors (FSCs) have gained increasing attention for their advantages including high power density and high storage density, allowing them to be operated even in extreme temperatures (Chen and Dai 2014; Choi et al. 2020; Shi et al. 2013; Wang et al. 2020).

FSCs are operated by accumulating the electrical charge in their electric double layer (EDL) (Chen et al. 2015; Hillier, Yong, and Beeby 2020). Thus, to enhance their electrochemical performance,

---

**CONTACT** Byungil Hwang ✉ bihwang@cau.ac.kr 🖵 School of Integrative Engineering, Chung-Ang University, Seoul 06974, Republic of Korea

increasing charge accumulation by enlarging the effective surface area of the electrode is crucial (Jia et al. 2007; Symeonidou et al. 2018; Xia, Yoshio, and Noguchi 2006). Moreover, the flexibility of the supercapacitor is mostly determined by the flexibility of the electrode (Jia et al. 2007; Lin et al. 2009). Choosing the right material for the FSC electrode, which should exhibit both a large surface area and high flexibility, is crucial (Cherusseri et al. 2020; Ma et al. 2022). Using porous materials with a large surface area enhances the electrochemical performance of the supercapacitor (Da Silva et al. 2020; Li et al. 2018). Carbon nanotubes (CNTs) meet the demands of FSC applications because of their aligned structure, excellent flexibility, high mechanical strength, outstanding electrical performance, high-rate capability, and electrochemical stability under cycling stress (Han et al. 2020; Kanoun et al. 2021; Kim et al. 2019; Mikhalchan and José Vilatela 2019; Sadiq et al. 2022; Sun et al. 2007; Wang et al. 2014). However, the low intrinsic specific capacitance of pristine CNTs limit their exclusive usage in developing flexible supercapacitor electrodes. There are various means of increasing the specific capacitance values of CNTs such as functionalization or compositing. For example, covalent functionalization modifies the surface properties of the CNTs, which changes the physiochemical properties. Park et al. demonstrated that the functionalization of carboxylic, sulfonic, and amine groups to the pristine MWCNTs resulted in the increase of specific capacitance value by two to fourfold (Park, Mahmood, and Seok Park 2013). Consequently, current research trends consider the incorporation of other materials such as conducting polymers, hydrogel, metal oxides, or other carbon materials into CNTs to maximize their desired properties (Gnanasekaran et al. 2017; Gregg, De Volder, and Baumberg 2022; Kanoun et al. 2021; Vashist et al. 2018). Therefore, in this review, we explain the fundamental structures and properties of single-walled CNTs (SWCNT), double-walled CNTs (DWCNT), and multi-walled CNTs (MWCNT). The fundamentals of flexible supercapacitors (FSCs) including the general device structure and operating mechanisms are discussed. Finally, the current trends of CNT (SWCNT, DWCNT, and MWCNT) applications to flexible supercapacitors are presented.

## Structure and properties of CNTs

CNTs are synthesized with a rolled-up graphene layer of carbon atoms arranged in the shape of a hexagon or pentagon (Iijima 1991; Lu and Chen 2005). As shown in Figure 1a–c according to the number of walls, CNTs can be categorized as (a) SWCNT, (b) DWCNT, and (c) MWCNT (Dai 2002; Pu et al. 2009). Differences in the structures result in different properties (Curtin and Sheldon 2004; Esawi et al. 2011). The typical diameters of SWCNTs, DWCNTs, and MWCNTs are approximately 1–2 nm (Sandanayaka et al. 2011), 2–5 nm (Ci et al. 2002), and 5–100 nm (Zaheer, Shamsuddin Jafri, and Sharma 2019), respectively.

A SWCNT is composed of only one graphene layer. The geometry of a SWCNT can be represented by the chiral indices (n, m), which show how the graphene sheet is oriented when rolling (Liu et al. 2017; Tange, Okazaki, and Iijima 2011). Understanding the chirality of SWCNTs is crucial because chirality plays a substantial role in electrical conductivity (Doh et al. 2019; Gaviria Rojas and Hersam 2020; Lian et al. 2016). The chiral vector $C_h$ depends on the chiral indices and the unit vectors $a_1$ and $a_2$, as shown in Equation (1) (Zhang, Yuan, and Tan 2011):

$$C_h = na_1 + ma_2 \tag{1}$$

In addition, the chiral angle $\theta$ (the angle between the vectors $C_h$ and $a_1$) determines the degree of twisting of the SWCNTs (Figure 1d) (Faria, Silvestre, and Canongia Lopes 2013; Joselevich 2006). As shown in Figure 1e, depending on the chiral angle, the SWCNT structures can be categorized into armchair ($\theta = 30°$), zigzag ($\theta = 0°$), and chiral structures ($0° < |\theta| < 30°$) (Ansari, Mirnezhad, and Sahmani 2013; Joselevich 2006; Zhang, Yuan, and Tan 2011). A gradual decrease is observed in the energy band gap as the chiral angle increases from 0° to 30°. Thus, the zigzag type of SWCNT shows semiconducting properties, whereas the armchair type
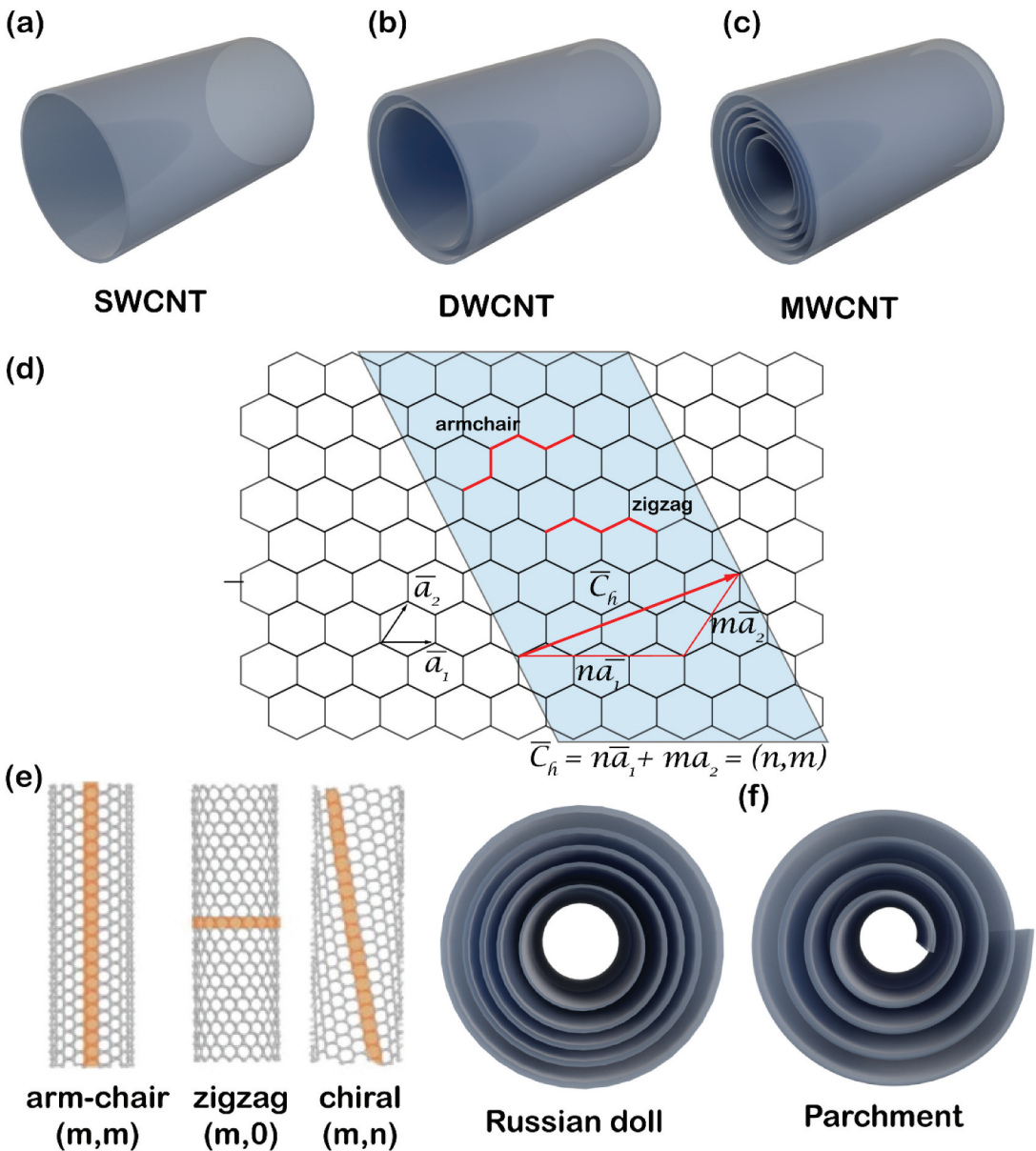
**Figure 1.** Surface and internal views of an (a) SWCNT, (b) DWCNT, and (c) MWCNT. Schematic representation of (d) the chirality parameters and (e) three structural types of CNT: armchair, zigzag, and chiral. (Boumia et al. 2014) (f) MWNT structural models: Russian Doll model (left) and Parchment model (right) (Gupta, Gupta, and Sharma 2019). Reproduced with permission from (Boumia et al. 2014) (Gupta, Gupta, and Sharma 2019).

of SWCNT shows metallic properties (Hároz et al. 2013; Pennington and Goldsman 2003; Zhou et al. 2004). Charoenpakdee et al. discovered the relationship between the chirality of the three different structures of SWCNT and the spin polarization of conductivity, using the Green-Kubo method. Chirality induced the asymmetric conductivity of the three types of SWCNT by causing a shift in the Diarc point. Beside the asymmetric conductivity, the chirality of SWCNTs also induces spin selectivity which produces different degrees of spin polarization. This spin polarization has a large impact on the temperature-dependent charge transport properties. Thus,

controlling the chirality of SWCNTs can optimize charge transport in SWCNTs (Charoenpakdee, Suntijitrungruang, and Boonchui 2020).

DWCNTs consist of two concentric SWCNTs (Moore, Tune, and Flavel 2015). The average diameter of a DWCNT is greater than that of an SWCNT (Laurent, Flahaut, and Peigney 2010; Pu et al. 2009). DWCNTs share the optimal electrical properties of both SWCNTs and MWCNTs (Benguediab et al. 2014; Shen, Brozena, and Wang 2011). Compared to SWCNTs, one of the advantages of DWCNTs is that the inner tube is well-protected by the outer wall (Di Bartolomeo et al. 2010; Kim et al. 2014; Li et al. 2005). Thus, the electrical and thermal properties of the inner tubes can be preserved under deformation conditions, exhibiting enhanced mechanical and thermal stability (Jeon et al. 2019; Tounsi et al. 2013). Similar to SWCNTs, the "individual chirality" of the tubes in DWCNTs also affects their electrical properties (Jeon et al. 2019; Kociak et al. 2002; Zhang and Shen 2008). However, the interaction between the inner tube and outer wall is a factor that affects the electronic properties of DWCNTs (Guillet et al. 2019; Kociak et al. 2002). DWCNTs are affected by both the interwall coupling strength and the average diameters of the inner and outer walls (Datta et al. 2011; Soto et al. 2015). A DWCNT can have one of four possible electronic configurations with each wall being either a semiconductor (S) or metallic (M) material: S@S, M@S, M@M, and S@M (inner-tube@outer-tube) (Moradian, Azadi, and Refii-Tabar 2007; Strano et al. 2003). As the diameter increases, the energy gaps of the S@S DWCNTs decrease and become gapless when the distance is greater than 1.5 nm. M@M DWCNTs always remain gapless. In addition, decreasing the distance between the walls leads to a change in the electronic structure. S@M DWCNTs exhibit a metallic behavior overall. Furthermore, if the two walls of S@S DWCNTs are far from each other, the overall DWCNT remains semiconducting. However, for a shorter interwall distance, DWCNTs become metallic. This behavior may be due to strong interactions among the 2pz orbitals, which are perpendicular to the cylindrical wall surface. By modifying the chirality of the inner/outer tubes and the distance between them, the overall electronic properties of DWCNTs can be modified according to the desired applications (Wei et al. 2003; Wu et al. 2021; Zólyomi et al. 2006). Thermal stability is another unique property of DWCNTs. DWCNTs are highly stable at temperatures up to 2000°C (Imazu, Fujigaya, and Nakashima 2015; Kim et al. 2014). DWCNTs can withstand much higher temperatures compared to SWCNTs. CNTs with narrow diameters tend to transform into CNTs with larger diameters, which are considered more stable (Jung et al. 2007; Lair, Herndon, and Murr 2008). This transformation can reduce the mechanical strain on the carbon atoms (Natsuki, Hayashi, and Endo 2006; Zhang, Tan, and Wang 2007). Basirjafari et al. analyzed the structural changes in DWCNTs, using Raman spectroscopy. RBM frequency is inversely proportional to the tube diameter. DWCNTs are stable up to 2000°C. When the temperature increases above 2200°C, the RBM peaks shift, suggesting an increase in the tube diameter and fragmentation of narrow nanotubes. The thermal stability of DWCNTs suggests their potential for use as electron field emitters operating at high currents (Basirjafari, Esmaielzadeh Khadem, and Malekfar 2013).

MWCNTs have two different structural models: the Russian Doll model and the Parchment model, depending on how the extra graphene sheets are layered (Eatemadi et al. 2014; Swetha 2022). As shown in Figure 1f, the Russian Doll model is arranged in consecutive layers of carbon nanotubes, whereas the Parchment model is rolled around itself, resembling a scroll of parchment (Gopalakrishnan et al. 2009). MWCNTs have similar properties as those of SWCNTs, except for the outer layer of the MWCNT protecting the inner layers from forming chemical interactions with external materials. Thus, MWCNTs exhibit improved tensile strength compared with SWCNTs (Kim et al. 2017; Montazeri et al. 2010). Young's moduli of SWCNTs have values around 1 TPa (WenXing, ChangChun, and WanZhao 2004). However, Young's moduli of MWCNTs were in the range of 270–950 GPa, indicating that MWCNTs have higher tensile strength than SWCNTs (Yeh, Hsieh, and Tai 2008). In addition, continuous bundles of MWCNTs have dozens of magnitudes lower tensile strength and Young's modulus than those of an individual MWCNT (Liew, Wong, and Tan 2006; Montazeri et al. 2010). Because of the unique geometry of MWCNTs, which consist of several layers of SWCNTs, they show distinct electronic properties (Lee et al. 2007; Park et al. 2005). The current flow

only occurs through the outermost layer of the nanotube (Yeh, Hsieh, and Tai 2008). The mutual interaction between the varying diameters of the nanotubes affects the band structure, similar to what happens with DWCNTs. The strong coupling interaction between the electronic states at the Fermi level and the phonon modes can cause superconductivity (Chen et al. 2018b; Kwon and Tománek 1998; Roche et al. 2001). However, the intrinsic defects of MWCNTs can degrade their electrical properties, indicating that not only the number of nanotube layers but also the quality of the MWCNT determines the overall electronic behavior (Chen et al. 2018a). Thus, purification processes are required prior to the synthesis of the materials (Domagała et al. 2019; Stobinski et al. 2010). Here, another merit of using MWCNTs is that their purification process is simpler and more cost-effective compared to those of SWCNTs or DWCNTs, making them versatile for application in diverse fields (Hou, Liu, and Cheng 2008; Ismail et al. 2008).

## Fundamentals of flexible supercapacitors

A supercapacitor exhibits a much higher capacitance value than conventional capacitors (An et al. 2002; Yang 2020). When a voltage is applied, the electric double layer is created in the supercapacitor, producing positive and negative charges between the interface of the electrolyte and electrodes (Kim, Matteini, and Hwang 2022). Then, the electrical charge is accumulated in this electric double layer (Zhao et al. 2015).

The materials used for supercapacitor electrodes can be categorized into electric double-layer capacitor (EDLC) types and pseudocapacitive types (Sinha and Kamal 2020). Carbon-based materials such as activated carbon, CNTs, and graphene are often considered EDLC types (Faraji and Nasir Ani 2015), whereas metal oxides, conducting polymers, and polymer composites are considered pseudo-capacitive types (Libich et al. 2018). The energy storage mechanisms differ between the two types of supercapacitors. As shown in Figure 2a, EDLCs store energy by the electrostatic accumulation of charge at the interface between the electrolyte and electrodes (Lei and Lekakou 2010). The porosity of the electrodes increases the charge accumulation by enhancing the penetration of the electrolytic solution into the pores of the electrodes (Mahankali et al. 2019). Therefore, using porous materials with a large surface area for producing the electrodes enhances the electrochemical performance of the supercapacitor (Celzard et al. 2002; Mahankali et al. 2019). By contrast, pseudocapacitors store energy through rapid surface redox reactions (Figure 2b) (Jiang and Liu 2019).

Among the two types of supercapacitors, the EDLC has gained increased attention as an energy storage device because of its high power density (Patil et al. 2020). Due to this high power density properties of EDLC, it can produce and store large amount of energy compared to its limited volume. The energy is stored and released via ion adsorption/desorption in EDLC mechanism, making EDLC possess high Coulombic efficiency, fast electric field response, and durability (Gao et al. 2015). Compared to conventional batteries, EDLC supercapacitors can store and release short-term power, owing to its high power density. Batteries, on the other hand, has high energy density, meaning that they can store energy for long term period (Xie et al. 2018).

The performance of a supercapacitor is determined by several factors including the types of current collectors, electrode materials, and electrolytes (Libich et al. 2018). Among these factors, the influence of the nature of the electrodes on the supercapacitor performance is substantial. Therefore, improving the properties of the electrode materials is as important as modifying the device configuration or the structures of the supercapacitors (Yu et al. 2015). The simplest means to improve the performance of the electrodes in EDLC is to increase the SSA of the electrode, which subsequently increases the overall capacitance (Salinas-Torres et al. 2019). Specifically, SSA refers to the total surface area of the different types of pores in the materials. Since higher SSA produces more active sites and promotes electrolytic diffusion, choosing the materials with high SSA can enhance the capacitance of the supercapacitor electrodes (Shi et al. 2021).

Adding to the excellent electrochemical performance of the supercapacitor, flexibility and mechanical stability under deformation are required as well (Shi et al. 2013; Wang et al. 2021).
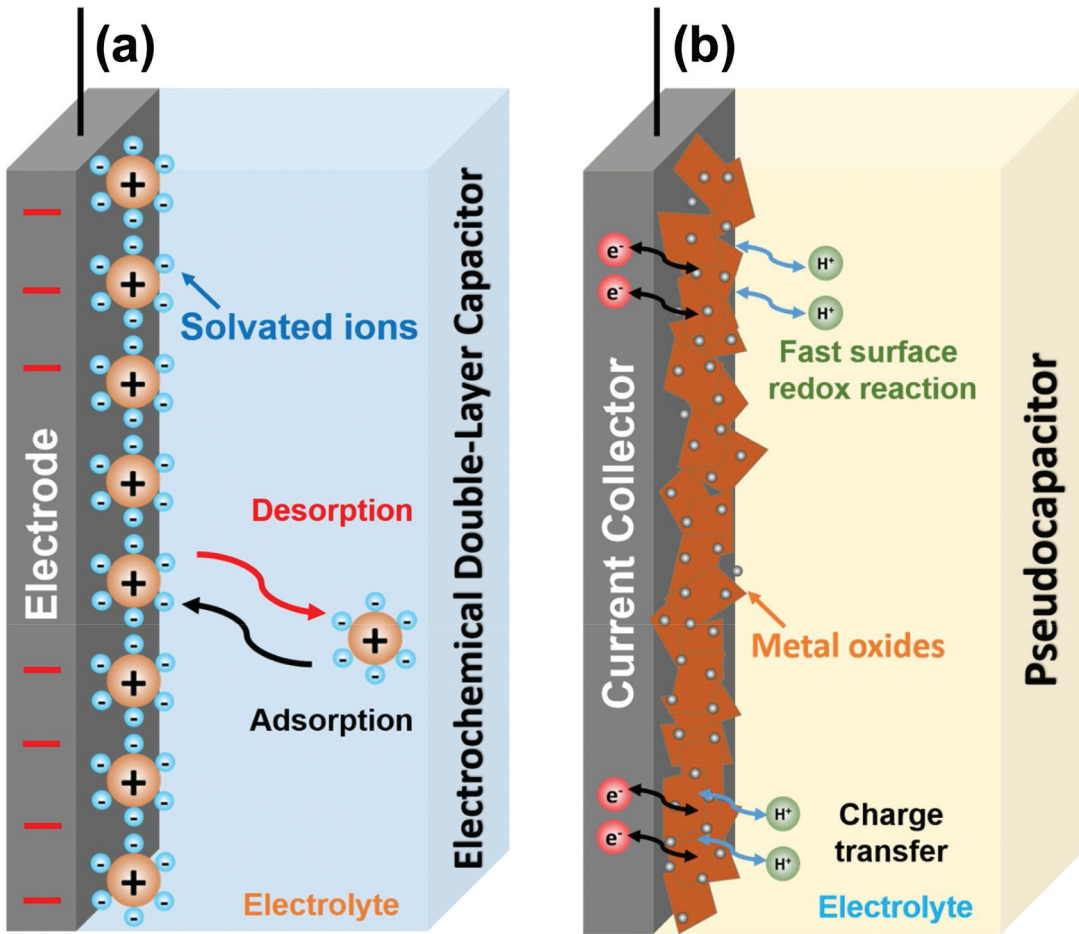
**Figure 2.** Comparison of charging mechanism of (a) EDLC type and (b) pseudocapacitor type. Reproduced with permission from (Wang, Zhu, et al. 2020).

Different types of stretchable supercapacitors using novel designs such as serpentines (Lee et al. 2019), kirigamis (Xu et al. 2018), and mesh structures (Wang et al. 2018) have been reported. However, these structural designs use brittle materials, which limit the cycling stability and mechanical strength under stress. CNTs are promising materials for stretchable supercapacitors because they satisfy the requirements mentioned above: high electrical conductivity, flexibility, high capacitance value, and mechanical strength (Lu 1997; Mintmire and White 1995; Odom et al. 2000; Popov 2004; Salvetat et al. 1999; Sun et al. 2002; Zaporotskova et al. 2016).

## Applications of CNTs to flexible supercapacitors

An aligned structure is one of the inherent properties of CNT (Yang et al. 2018). This property makes CNT a promising candidate for stretchable electrode materials that can be applied to flexible supercapacitors. CNTs not only show excellent flexibility (Yang et al. 2018), mechanical strength (Ryu et al. 2015), and outstanding electrical performance (Kim et al. 2017) but also exhibit high-rate capability and maintain their electrochemical stability under cycling stress (Tian et al. 2019). The requirements for EDLC electrodes not only include high surface area but also require rapid charge/discharge rate
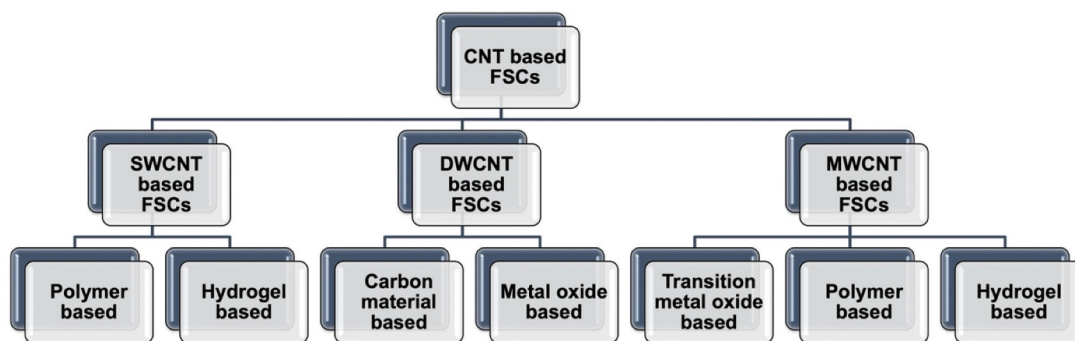
**Figure 3.** Types of electrode materials for producing flexible supercapacitors (FSCs).

(Ike, Sigalas, and Iyuke 2016), large potential window (Likitchatchawankun et al. 2021), and high conductivity (Aziz et al. 2020). CNTs can thus satisfy the requirements needed to enhance the EDLC properties. In this review, we categorized the CNT-based flexible supercapacitors according to the structural types of CNTs: SWCNTs, DWCNTs, and MWCNTs as shown in Figure 3.

### SWCNT-based flexible supercapacitor electrodes

SWCNTs have relatively high surface area, making them ideal candidates for supercapacitor electrodes (Kobashi et al. 2011). SWCNTs also exhibit a high Young's modulus of elasticity and tensile strength, preserving their electrochemical performance under external deformation (Agrawal et al. 2006; Parvaneh and Shariati 2011). Moreover, they have relatively higher specific capacitance values compared to DWCNTs and MWCNTs, enhancing the energy and power density of the supercapacitor (Shiraishi et al. 2002; Zhang, Yuan, and Tan 2011).

### Polymer/swcnt-based supercapacitor electrodes

Because of the environmental problems caused by utilizing inorganic materials for making super-capacitor electrodes (Peng, Jin, and Chen 2007), organic electroactive materials (Peng, Jin, and Chen 2007) are gaining attention for their applicability to stretchable electrodes. Samy et al. proposed conjugated microporous polymers (CMPs) with the use of SWCNTs for fabricating high-performance supercapacitor electrodes (Samy et al. 2021). A CMP is a type of porous organic polymer that shows many attractive characteristics including a high surface area, porosity, and facile fabrication (Weber and Thomas 2008). However, a CMP cannot be used alone because of its low conductivity (Wang et al. 2017). As shown in Figure 4a, Samy et al. simply blended tetrabenzonaphthalene (TBN)-based CMPs with SWCNTs (2 wt.%) applying the Sonogashira-Hagihara cross-coupling method to synthesize TBN-CMP/SWCNT nanocomposites for constructing supercapacitor electrodes. The electrochemical performance of the TBN-CMP/SWCNT material was analyzed using a three-electrode system with 1 M aqueous KOH as the electrolyte. The addition of SWCNT to TBN-CMP enhanced the overall electrochemical performance of the fabricated supercapacitor. Especially, the highly porous structure of SWCNT resulted in producing a diffusion channel and allowed efficient electrolyte ion transport, increasing the capacitance value. In Figure 4b, the CV profiles at sweep rates from 5 to 200 $mVs^{-1}$ were measured and the curves showed rectangular shapes, indicating their capacitive responses were of the EDLC type (Lukatskaya, Dunn, and Gogotsi 2016). The GCD curves showed triangular shapes, indicating both pseudocapacitive and EDLC behaviors (Figure 4d). The discharging times were longer with the addition of SWCNT, which proves that the SWCNT enhanced the overall capacitance. The calculated specific capacitances of the TBM-Py-CMP/SWCNT, TBN-TPE-CMP /SWCNT, and TBM-Car-CMP/SWCNT materials at a current density of 0.5 $Ag^{-1}$ were measured as 430, 156, and 53 $Fg^{-1}$ (Figure 4c). Compared to the materials without SWCNT, the values increased
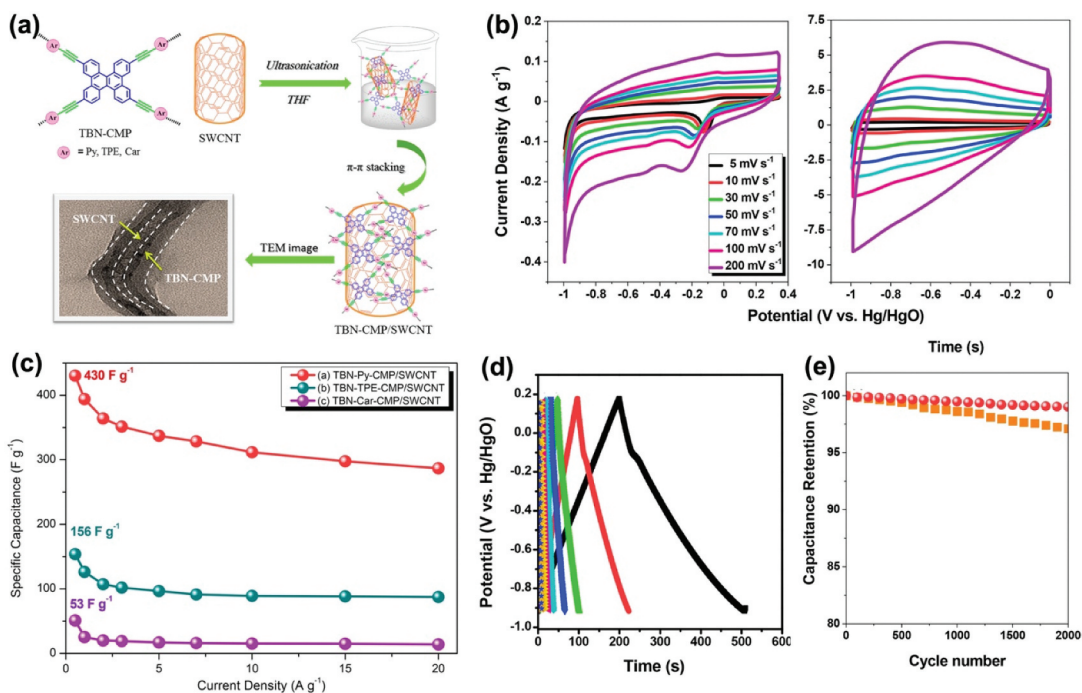
**Figure 4.** (a) Schematic diagram of the manufacture of TBN-CMP/SWCNT nanocomposites and TEM images. (b) CV curves of TBN-Py-CMP (left) and the TBN-Py-CMP/SWCNT composite (right). (c) Specific capacitance profiles of the composites with SWCNTs added at various current densities. (d) GCD curves of TBN-CMP/SWCNT at various currents. (e) Cycling stabilities of TBN-Py-CMP and the TBN-Py-CMP/SWCNT composite, measured at 10 Ag$^{-1}$ over 2000 cycles. Reproduced with permission from (Samy et al. 2021).

14-fold. The high porosity of SWCNT allows for more efficient transport of electrolyte ions by providing diffusion channels, which consequently enhances the capacitance (Wimalasiri and Zou 2013). The cyclic stability was also estimated at a current density of 10 Ag$^{-1}$. The capacitance retention after 2000 cycles for TBM-Py-CMP/SWCNT was measured as 99.18% (Figure 4e). The enhanced cyclic stability was attributed to the excellent performance of the fabricated supercapacitor electrode because of the strong π-stacking between the TBN-Py-CMP and SWCNTs (Samy et al. 2021).

Shokry et al. fabricated a supercapacitor electrode based on a poly (3-hexylthiophene) (P3HT)/SWCNT nanocomposite. P3HT is a conducting polymer and is considered a promising material because of its pseudocapacitive behavior, high electrical conductivity, and high energy density (Shokry et al. 2022). When SWCNT is blended with P3HT, it can store charges in the electrical double layer. Shokry et al. tested the fabricated P3HT/SWCNT electrode in a three-electrode system with a 0.1 M LiClO$_4$ electrolyte. The CV curve exhibited a stable shape with a single oxidation peak at 1.0 V and a single reduction peak at 0.6 V, indicating the Faradic pseudocapacitive characteristic of the electrode (Figure 5a). In addition, as shown in Figure 5, the current increases with the scan rate while preserving the overall shape of the CV curve, which indicates a high electrical capacity. Adding SWCNTs increased the area of the CV curve because of the intrinsic EDLC characteristics of carbon materials (Wimalasiri and Zou 2013). In Figure 5b, the GCD curves show semisymmetric triangular shapes, indicating the pseudocapacitive and EDLC characteristic of SWCNTs. The specific capacitance of SWCNT added to P3HT nanocomposites at 0.5 Ag$^{-1}$ was 254.8 Fg$^{-1}$, which increased greatly compared to the pristine P3HT, which indicated 160.5 Fg$^{-1}$. The capacitance retention was 80.5% after 1000 cycles, proving long-term cycle stability (Figure 5c).

Zhang et al. introduced another type of composite materials, poly(3,4-ethylenedioxythiophene) (PEDOT) with SWCNT as the electrode material in supercapacitors (Zhang et al. 2020). PEDOT not only shows high conductivity (>500 Scm$^{-1}$) but also has excellent redox activity and
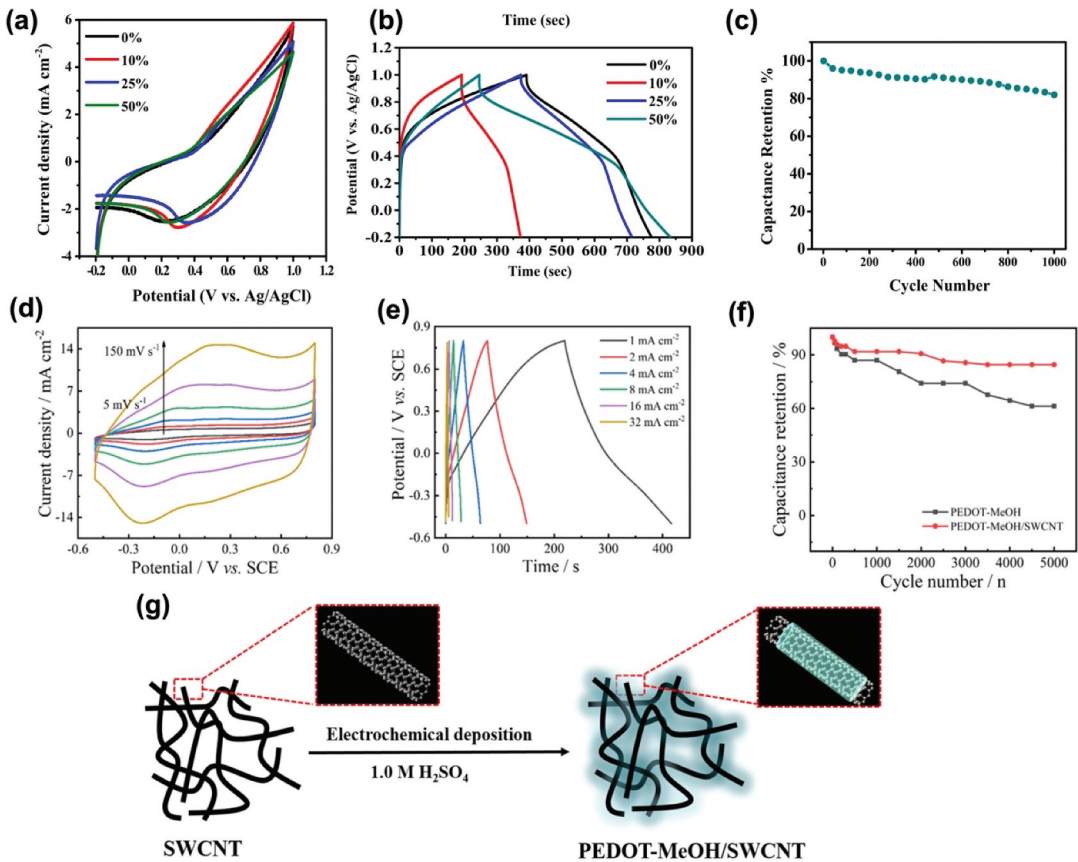
**Figure 5.** (a) CV curves of P3HT/SWCNT electrodes with different SWCNT ratios at 50 mVs-1 (Shokry et al. 2022). (b) GCD curves of P3HT/SWCNT electrodes with different SWCNT ratios at 0.5 Ag-1 (Shokry et al. 2022). (c) Cycling stability of the P3HT/50% SWCNT nanocomposite supercapacitor electrode at 1 Ag$^{-1}$ for 1000 GCD cycles (Shokry et al. 2022). (d, e) CVs and GCD of PEDOT-MeOH /SWCNT (Zhang et al. 2020). (f) Cycling stability of PEDOT-MeOH and PEDOT-MeOH/SWCNT nano-network (Zhang et al. 2020). (g) Schematic illustration of the preparation of the PEDOT-MeOH/SWCNT nano-network (Zhang et al. 2020). Reproduced with permission from (Shokry et al. 2022; Zhang et al. 2020).

mechanical stability (Zhang et al. 2015). However, PEDOT exhibits a low specific capacitance of 80–120 Fg$^{-1}$, which makes it difficult to use it alone (Lota, Khomenko, and Frackowiak 2004). To overcome this problem, methanol (MeOH) was added to PEDOT to increase the solubility by conjugation of the PEDOT chain, while lowering the initial oxidation potential and the band gap of PEDOT (Zhang et al. 2020). Herein, by adding SWCNTs, the current densities increased due to the high electronic conductivity of SWCNTs (Peng, Jin, and Chen 2007). Thus, Zhang et al. prepared a homogenized PEDOT-MeOH/SWCNT nano-network, using the electrochemical co-deposition method that can be applied to supercapacitors with using electrolyte as 1 M H$_2$SO$_4$ solution. The tubular morphology of SWCNTs were maintained as hard template and PEDOT-MeOH was deposited to the template as shown in Figure 5g. PEDOT-MeOH/SWCNT exhibited CV curves with a steady shape, even when a high scan rate of 150 mVs$^{-1}$ was used, indicating high kinetic reversibility (Figure 5d). When SWCNT was added, the redox peaks were more pronounced, and the peak current density increased at a higher rate with increasing scan rates. This was attributed to the high electric conductivity and rapid reversible redox reaction of SWCNTs. The GCD curve was slightly different from that of the conventional EDLC, exhibiting deviations from linearity, which were due to the pseudocapacitive behavior of PEDOT-MeOH (Figure 5e). The calculated specific capacitance at 1.0 mAcm$^{-2}$ increased from 49.6 to 151.2

mFcm$^{-2}$. The cycling stability of the fabricated PEDOT-MeOH/SWCNT electrode was tested for 5000 cycles. Figure 5f shows that the addition of SWCNTs increased the capacitance retention from 61.3% to 84.5% after 5000 cycles. Moreover, Zhang et al. proved that this high capacitance retention was maintained even with different types of electrolytes (Zhang et al. 2020).

Zhou et al. utilized a new type of conducting polymer (polythiophene), which shows high redox states and high charge mobility. When this polythiophene is blended with SWCNTs, the high specific surface area of SWCNTs enhanced the exposure of this hybrid electrode material to the electrolyte by the action of the graphite planes or edges. The surface modification of SWCNTs with a poly(3-oligo(ethylene oxide))thiophene was conducted by esterification. As shown in Figure 6a, the hydrophilic properties of the ethylene oxide groups improved the overall polarity of the material, facilitating the penetration of the PVA/KCl gel electrolyte. Moreover, the flexible oligo (ethylene oxide) groups provided enough space for volumetric changes, preventing further damage during the charge-discharge processes. The CV curves of the PD2ET-g-SWCNT sample displayed larger profile areas compared to those without SWCNTs, indicating that the former shows higher specific capacitance (Figure 6b). Zhou et al. identified the factors behind the enhanced electrochemical properties as the oligo (ethylene oxide) groups, which improved the hydrophilic characteristics and thus facilitated the rapid access of the electrolyte ions to the surface of the SWCNTs. The symmetric shapes of the GCD curves in Figure 6c show a linear relation of discharge/charge versus time. This suggests not only high electrochemical capacity but also reversibility. Furthermore, the PD2ET-g-SWCNTs maintained a high current density, avoiding a visible ohmic drop. This also proves the highly reversible charge transfer in the fabricated electrode. The calculated specific capacitance from the GCD curves was 399 F/g at a current density of 1 A/g. The sample without SWCNTs
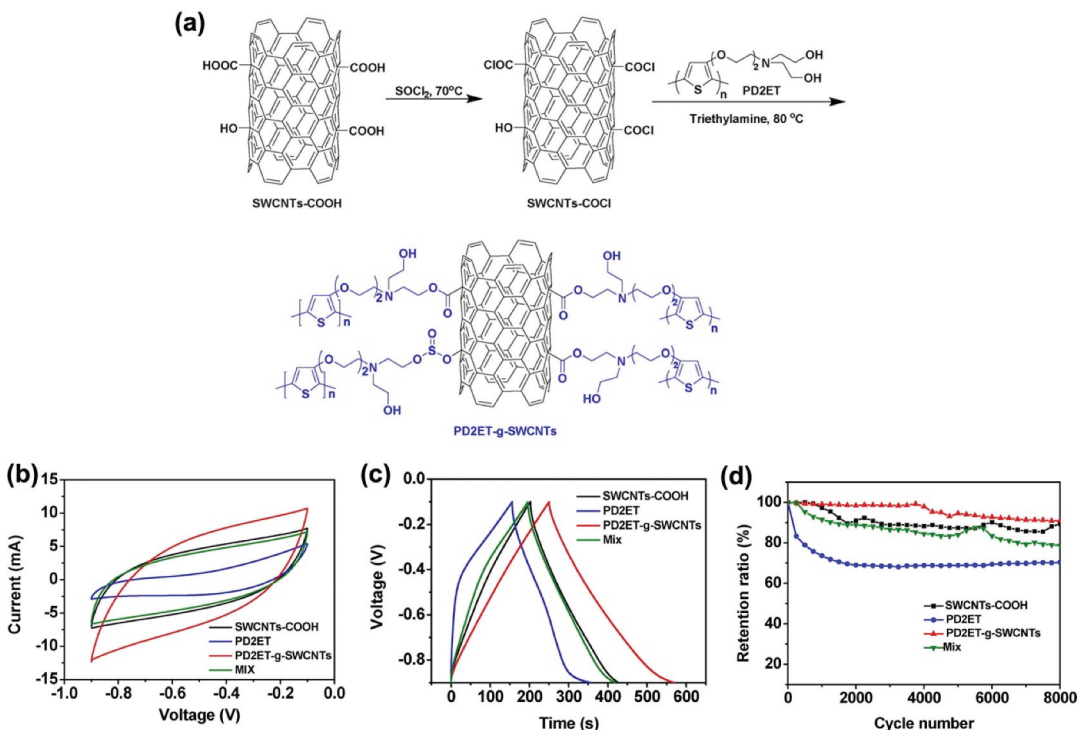


Figure 6. (a) Synthesis scheme for the preparation of PD2ET-g-SWCNT hybrids. (b) CV curves of PD2ET-g-SWCNTs at different scan rates. (c) GCD curves for four electrodes at a current density of 1.0 A/g. (d) Cycle stability of four electrodes at 100 mV/s for 8000 CV cycles. Reproduced with permission from (Qian et al. 2019).

showed around 250 F/g of specific capacitance. The cycling stability indicated up to 8000 cycles at 100 mV/s. The capacitance retention was highly stable for the first 4000 cycles but decreased after 80,000 cycles (Figure 6d). However, the decreased value of the capacitance retention was 91%, which can still be considered superior cycling stability. Zhou et al. attributed this result to the PD2ET covalent grafting to SWCNTs, which prevented structure pulverization and provided sufficient diffusion channels for the volumetric changes during the charge/discharge process (Zhou et al. 2019).

### Hydrogel/swcnt-based supercapacitor electrodes

Hydrogels are 3D hydrated mesh materials with multiple building blocks. They are considered promising materials in the field of energy conversion and storage systems. Hydrogels not only have a large specific surface area and a high porosity but also exhibit hydrophilic mechanical elasticity. Hydrogels have the advantages of reversibility and tunability, so they can be applied in various energy storage devices that can be stretched or bent. Moreover, when hydrogels are combined with carbon-based materials, their structural advantages can be maximized. The 3D-interconnected porous-percolating network allows for rapid ion transfer, which enhances electrical conductivity compared to the pristine hydrogel.

Badawi et al. synthesized a cotton-based high-conducting SWCNT/PEDOT:PSS/hydrogel-based supercapacitor. The fabricated supercapacitor exhibited high capacity and flexibility. SWCNT/PEDOT:PSS was coated on the cotton fabric through the dip-coating method. Since cotton itself has high porosity, the prepared ink solution was absorbed well. Poly(acrylamide)/Na-alginate hydrogel electrolytes were synthesized by the polymerization process. SWCNTs are visible in the coating and are non-uniformly scattered on the surface of the cotton fibers. The interconnected SWCNTs forms a thick system that allows for an exchange of current transmission along the surface. The symmetric supercapacitor cell was prepared in a sandwich structure where the hydrogel electrolyte was surrounded by the SWCNT/PEDOT:PSS-coated cotton fabric (Figure 7a). The capacitive behavior of the SWCNT/PEDOT:PSS/hydrogel-based supercapacitor was analyzed using the CV curve. As shown in Figure 7b, the fabricated cotton-based capacitor had a large CV area. The specific capacitance was 212.16 F/g at 50 mV/s. Badawi et al. highlighted that the complete dissociation of SWCNT in a PEDOT:PSS solution causes an increase in ionic transport, leading to higher specific capacitance. The fabricated aerogel film exhibited a rectangular curve at a high scanning rate, indicating a strong charge transfer ability and rate capability. The GCD curve also maintained a regular triangular shape, suggesting high voltage resistance. The specific capacitance was 605.32 $mF/cm^2$ at 2 $mVs^{-1}$. The cycling stability of the film was measured at a current density of 2.87 $mA/cm^2$. The capacitance retention was measured as 91.9% even after 10,000 cycles. The electrochemical performance of the fibrous network structure was preserved even after bending or compressing, which can cause structural deformation (Badawi et al. 2023).

Chang et al. developed a $MoS_2$ nanosheet/SWCNT/cellulose nanofibril hybrid aerogel film for supercapacitors with PVA/$H_2SO_4$ gel electrolyte. Molybdenum disulfide ($MoS_2$) is a type of transition metal sulfide with a layered structure. $MoS_2$ is an electrode material applicable to supercapacitors because it can store charges on the surface and in between the layers by the reversible insertion of electrolyte ions. However, using $MoS_2$ alone is difficult because it has low conductivity and agglomerates during the insertion/disinsertion process, which deteriorates the cycle performance of the supercapacitors. Thus, adding SWCNTs can prevent the agglomeration of $MoS_2$ nanosheets by increasing the layer space. The bonding between the SWCNTs and $MoS_2$ is weak, reducing the flexibility of the electrodes. To make the composite electrodes more flexible, cellulose nanofiber (CNF) was added to form a hydrogen bond between the SWCNTs and $MoS_2$, enhancing the mechanical strength and stability. Figure 7c shows the schematic diagram of the preparation of a $MoS_2$-SWCNT/CNF aerogel film by the hydrogen bond cross-linking method. The fabricated samples all exhibited high cycle reversibility (Figure 7d). Moreover, as the amount of SWCNTs added increased, the CV curve exhibited the characteristics of both EDLC and pseudocapacitance.
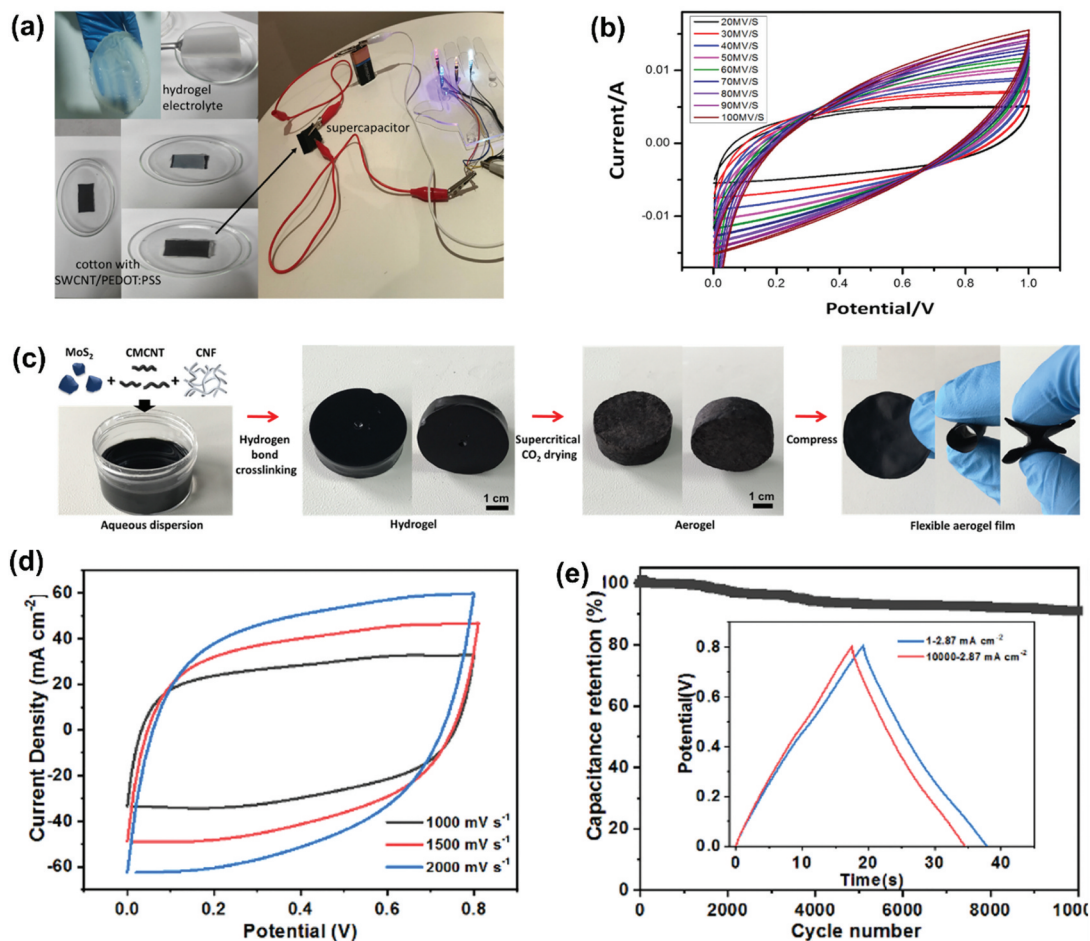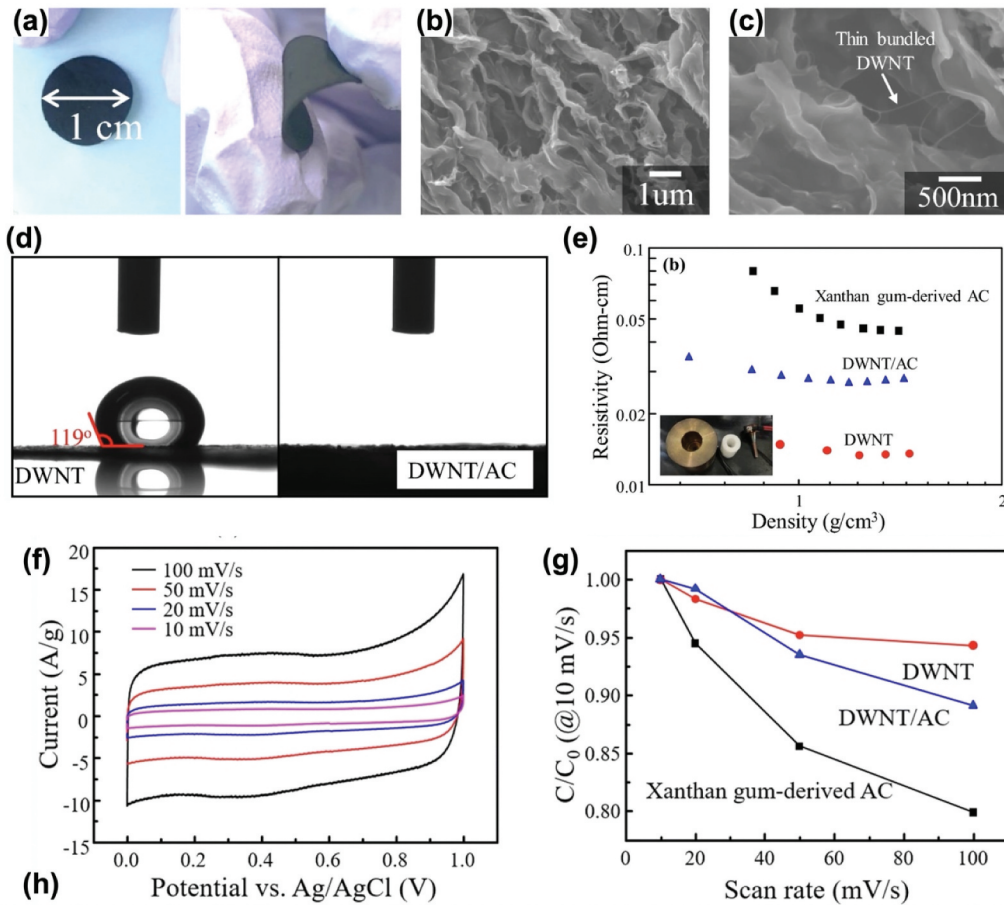
**Figure 7.** (a) Setup device fabrication by connecting two cotton SWCNT/PEDOT:PSS electrodes with a hydrogel electrolyte (Badawi et al. 2023). (b) CV curves of an SWCNT/PEDOT:PSS/hydrogel electrolyte-based supercapacitor (Badawi et al. 2023). (c) Schematic diagram of the fabrication of a $MoS_2$-SWCNT/CNF flexible aerogel film (Chang et al. 2022). (d) CV curves of a $MoSCF_3$ supercapacitor electrode at high scanning rates (Chang et al. 2022). (e) Cyclic stability test of a $MoSCF_3$ supercapacitor electrode (inset: the GCD curve before and after 10,000 charge and discharge processes) (Chang et al. 2022). Reproduced with permission from (Badawi et al. 2023; Chang et al. 2022).

The cycle stability of $MoSCF_3$ was tested and the specific capacity was maintained at 91.01% of its initial value after 10,000 cycles (Figure 7e) (Chang et al. 2022).

## DWCNT-based flexible supercapacitor

### Carbon material/DWCNT-based supercapacitor electrodes

Activated carbon (AC) is a promising material for conventional supercapacitors owing to its large specific surface area, chemical durability, low cost, and wide electrochemical window. AC is generally used with other conductive fillers instead of being used alone. However, the problem with this mixture of AC and conductive fillers is that their electrical resistance is too high to be applied for supercapacitor applications. To overcome this issue, DWCNTs have been used to enhance the electrochemical performance of AC-based electrodes. Kang et al. spread a stable DWCNT suspension into a thin film and dispersed it within the AC. These authors fabricated a free-standing electrode with a large surface area and high specific capacitance. Xanthan gum was prepared as a dispersing agent for

**Figure 8.** (a) Photograph showing a flexible and free-standing thin film consisting of DWNTs and xanthan gum-derived activated carbon. (b) and (c) SEM micrographs showing the pleated structure and thin bundled DWNTs between two adjacent pleats. (d) Water contact angles of pure DWNTs and DWNT-filled activated carbon composite. (e) Electrical resistivity of the pure DWNTs, xanthan gum-derived activated carbon, and DWNT-filled activated carbon composite in the bulk state using a two-probe system. (f) Cyclic voltammograms of DWNTs filled with activated carbon at different scan rates for the applied potential. (g) Rate capabilities of the three samples. (h) Table of the pore structure, electrical resistivity, and specific gravimetric capacitance of xanthan gum-derived activated carbon, pure DWNTs, and DWNT-filled activated carbon composite. Reproduced with permission from (Kang et al. 2020).

the DWCNT suspension. The carbonized sample was chemically activated to obtain a carbon-coated DWCNT suspension. One of the intrinsic properties of the DWCNT is the strong van der Waals interaction between the tubes, causing large-sized bundles. Therefore, using xanthan gum for dispersing the aggregated DWCNTs is necessary. Figure 8a shows the thin xanthan gum film coating the DWCNT suspension and its microscopic structure is also shown by SEM with different resolutions (Figures 8b–8c). Thin bundled DWCNTs were observed between the activated carbons, demonstrating homogeneous dispersion.

The hydrophilicity of the fabricated electrode was verified by measuring the contact angle of the pure DWCNTs and DWCNT/AC (Figure 8d). The contact angle of the DWCNT/AC could not be measured because of the abrupt disappearance of the water, while that of the pure DWCNT was 119°, indicating its hydrophobicity. The main reason for DWCNT/AC exhibiting hydrophilicity is the high ratio of oxygen atoms that come from xanthan gum-derived AC, which is placed on the surface of the DWCNTs. The hydrophilic nature of the electrode helps supercapacitors to attain higher specific capacitance. Moreover, the change in the electrical resistivity of the pure DWCNTs, xanthan gum-derived AC, and DWCNT-filled AC composite was measured (Figure 8e). The fabricated DWCNT/AC composite exhibited electrical resistivity between the two single fillers. The homogeneously dispersed DWCNTs acted as electrical conductors, lowering the resistivity. The electrochemical performance was measured using a three-electrode cell with a 1 M $H_2SO_4$ solution as an electrolyte. As shown in Figure 8f, the obtained CV curves displayed a quasi-rectangular shape, indicating an ideal capacitive behavior and non-Faradaic double-layer reaction. The specific capacitance of the xanthan gum-derived AC decreases as the scan rate increases because of its low electrical conductivity. However, DWCNT/AC exhibits high-rate performance, owing to its high electrical conductivity (Figure 8g). Compared to the pure DWCNT or xanthan gum-derived AC, the specific capacitance of DWCNT/AC is much higher at any scan rate (Figure 8h). Kang et al. provided three possible reasons for this phenomenon: (1) the large increase in the micropore volume contributing to the capacitive performance, (2) the relatively higher electrical conductivity of DWCNT/AC compared to that of xanthan gum-derived AC, and (3) the hydrophilicity of DWCNT/AC that allows the aqueous electrolyte to seep into the pores (Kang et al. 2020).

In addition to AC, graphene is often used as a hybrid structure with DWCNTs. Owing to its high surface area, high electrical conductivity, and superior electrochemical characteristics, a graphene/CNT hybrid structure can be applied to diverse fields including energy storage devices, sensors, and fuel cells. This type of graphene/CNT hybrid structure is composed of a graphene sheet placed on the side of the CNT in $H_2SO_4$ electrolyte. To maximize the electrochemical performance of the graphene/CNT hybrid structure, Muangrat et al. proposed nitrogen doping by inducing pseudocapacitive characteristics. The specific capacitance of the fabricated nitrogen-doped graphene nanosheet-grafted DWCNT (NG-DWCNT) was measured as 563 F/g at 50 A/g. The CV curves exhibited a quasi-rectangular shape. The nitrogen doping on the graphene/DWCNT hybrid structure increased the area of the CV curve. The synergistic effect of the hybrid structures with graphene edges and nitrogen doping improved the overall electrochemical properties. In addition, the cyclic stability was tested at a current of 0.5 mA for 5000 cycles. The capacitance retention of the NG-DWCNT (94.35%) was mostly preserved even after 5000 cycles, suggesting the superior cyclic stability of the fabricated sample (Muangrat et al. 2021).

### *Metal-organic frameworks (MOFs)/DWCNT-based supercapacitor electrodes*

Na et al. developed an "all-in-one" fiber with a hybrid composite comprising a DWCNT yarn and metal-organic frameworks (MOFs). The main goal of fabricating this fiber was to achieve both electrical conductivity and mechanical stability. DWCNTs are known to exhibit high electrical conductivity (14,310 $Scm^2g^{-1}$), making them excellent materials for energy storage systems. Additionally, high specific surface area and porosity of DWCNTs enhance both mechanical and electrochemical performance of supercapacitors. The structure of the fiber was designed to decorate the surface of the strong and conductive DWCNT yarn with MOF-derived carbons (MDCs). The hybrid composites were developed by spinning the DWCNTs and combining them into a single fiber with considerable thickness as shown in Figure 9a. Then, the isoreticular MOF-1 (IRMOF-1) was decorated on the surface of the DWCNT yarn in a jewel-like fashion. The SEM images in Figures 9b , and c demonstrate the morphology of the MDC beads attached to the DWCNT yarn. This structure increases the exposure of the highly porous carbon, which functions as a high-energy storage system.
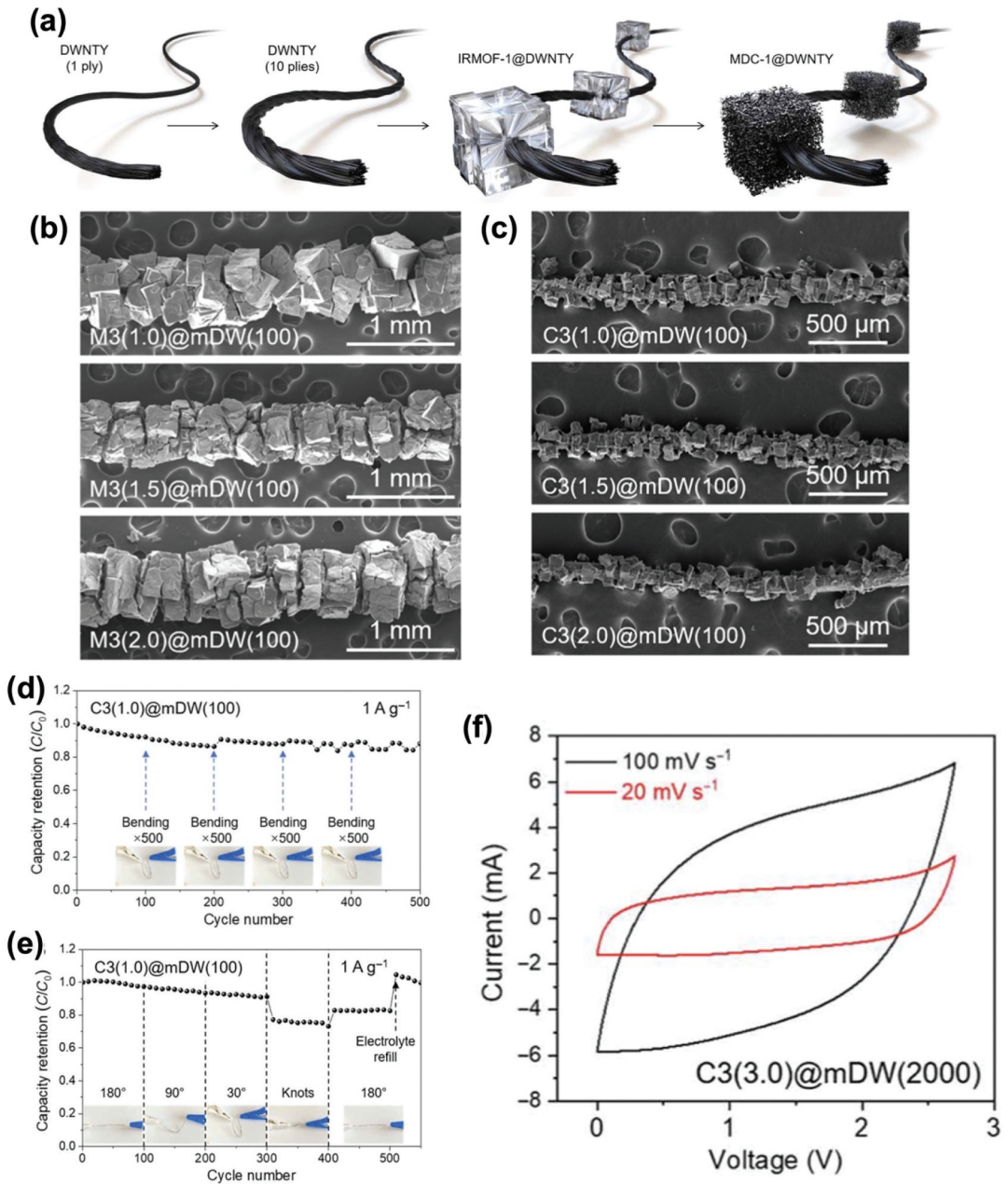
**Figure 9.** (a) Schematics illustrating the synthetic process to prepare a thickened hybrid composite of DWCNT and MOFs. (b) and (c) SEM images at different precursor concentrations with different resolutions. Cycle performance of the hybrid composite-based all-solid-state supercapacitor under (d) cumulative bending and (e) at different bending angles at 1 Ag$^{-1}$. (f) CV curves of the hybrid composite-based supercapacitor. Reproduced with permission from (Na et al. 2022).

The fabricated hybrid composite of DWCNT and MOFs with polyvinyl alcohol–dimethyl sulfoxide (PVA-DMSO) gel electrolyte was evaluated for its mechanical stability under extreme conditions. As shown in Figure 9d, the DWCNT/MOF-based supercapacitor exhibited a capacitance retention of 88.0% after 500 cycles, indicating negligible mechanical deformation after repeated bending. This result verifies the remarkable flexibility of the supercapacitor. Moreover, the energy storage

performance did not decline at various bending angles (Figure 9e). When the fiber was knotted, the capacity retention deteriorated; however, the capacitance was regained after recovery, demonstrating the mechanical reliability of the material. Figure 9f shows the quasi-rectangular shapes of the CV curves of the supercapacitor, confirming the EDLC behavior. The developed hybrid composite had a high volumetric capacitance of 225.2 $F/cm^3$ and a specific capacitance of 151.1 $Fg^{-1}$ at 1 $Ag^{-1}$. Its tensile strength was measured as 492.8 MPa and the stable cycle performance under repetitive bending confirmed the mechanical robustness of the supercapacitor (Na et al. 2022).

### MWCNT-based flexible supercapacitor

MWCNTs have several advantages over SWCNTs and DWCNTs. Preparing MWCNTs with high purity requires less strict conditions, which makes them versatile in various fields compared to SWCNTs and DWCNTs. For instance, the catalyst size for chemical vapor deposition (CVD) can be large, and some synthetic methods such as arc discharge and laser ablation, do not require the use of a catalyst. Obtaining MWCNTs with high purity is crucial because capacitance increases with higher purity. Another advantage is attributed to the structure of MWCNTs. Due to the presence of an outermost wall, the inner layers can remain intact under deformation ("sword-in-sheath" failure). Thus, the structural defects that cause a decrease in the tensile modulus can be prevented. The one-dimensional carbon structure of the MWCNT is also different from that of the SWCNT. SWCNTs are either semiconducting or metallic depending on their chiral vector. However, MWCNTs consist of several layers of nanotubes, making them electrically conductive in both the radial direction and nanotube axis orientation. In particular, at a sufficiently high temperature, MWCNTs exhibit properties that are intermediate between metallic and semiconducting properties. Moreover, like SWCNTs and DWCNTs, MWCNTs exhibit a high tensile modulus and mechanical robustness. MWCNTs have Young's moduli values of around 1.8 TPa, being much higher than those of other carbon materials. Young's modulus increases with less than 1 wt.% of MWCNT loading. However, with high loading, the strength is deteriorated because of nanotube agglomeration. Thus, it is also important to determine the ideal loading of MWCNTs. These advantages of MWCNTs allow them to be applied to other various materials including polymers, hydrogels, and transition metal oxides.

### Metal oxide/MWCNT-based supercapacitor electrodes

Although MWCNTs show high electrical conductivity, high power density, and a rapid rate of charge and discharge, making them promising EDLC materials for supercapacitor electrodes, they need to overcome the challenges of having low energy density. Unlike MWCNTs, pseudocapacitive metal oxides such as $MnO_2$ or $RuO_2$ exhibit higher energy density than EDLC materials. However, the slow Faradaic reaction of pseudocapacitive materials lowers their power density. Moreover, metal oxides show low electrical conductivity, which hinders their independent use as supercapacitor materials. Thus, using both porous carbon materials (which have EDLC properties) and metal oxides (which have pseudocapacitive characteristics) simultaneously is the current trend for supercapacitor electrode materials.

Aruchamy et al. introduced $ZnMn_2O_4$, a type of binary metal oxide, which has a wide potential window, excellent conductivity, and high mechanical strength. However, $ZnMn_2O_4$ shows poor electrical conductivity. Aruchamy et al. expected the synergistic effects of $ZnMn_2O_4$ and MWCNTs to complement each other. To enhance the electrical properties of MWCNTs, Aruchamy et al. performed acid modification with a mixture of $H_2SO_4$ and $HNO_3$. Lau et al. verified the effect of MWCNT functionalization by acid treatment on electrical conductivity. MWCNTs with high electrical conductivity can be used to improve the conductivity of metal oxides as well decreasing resistivity. The $ZnMn_2O_4$/MWCNT composite was fabricated using a one-step hydrothermal method, which avoided complicated processes. The fabricated $ZnMn_2O_4$/MWCNT composite with $Na_2SO_4$ electrolyte demonstrated the effect of adding MWCNTs to the pure $ZnMn_2O_4$ electrodes (Figure 10a).
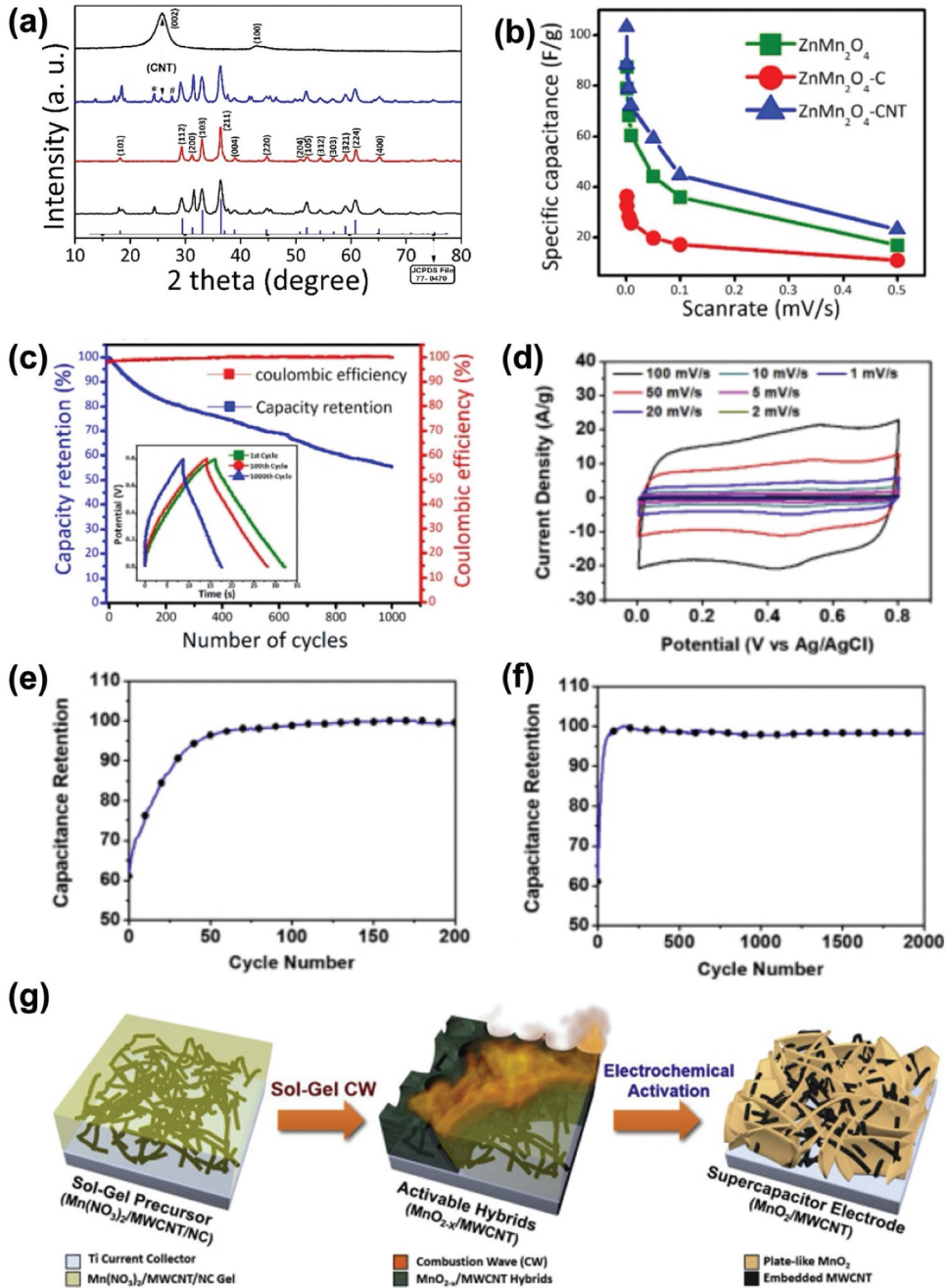
**Figure 10.** (a) XRD patterns of ZnMn$_2$O$_4$, ZnMn$_2$O$_4$-C, ZnMn$_2$O$_4$-CNT, and pristine MWCNTs (from bottom to top) (Aruchamy et al. 2020). (b) Scan rate-dependent specific capacitances (Aruchamy et al. 2020). (c) Cycle number versus capacity retention and Coulombic efficiency of ZnMn$_2$O$_4$-CNT (Aruchamy et al. 2020). (d) CV curves of MnO$_2$/MWCNT electrodes (Aruchamy et al. 2020). (e) Normalized capacitances of initial cycles until 200 cycles (Shin et al. 2019). (f) Normalized capacitances of full activation within 2000 cycles (Shin et al. 2019). (g) Schematic of sol-gel-driven combustion wave (CW) for one-step fabrication of MnO$_{2-x}$/MWCNT hybrids (Shin et al. 2019). Reproduced with permission from (Aruchamy et al. 2020; Shin et al. 2019).

The maximum specific capacitance of the $ZnMn_2O_4$/MWCNT composite was 103 F/g at 1 mV/s scan rate, while that of the pure $ZnMn_2O_4$ electrode was 87 F/g at the same scan rate (Figure 10b). This improvement in the specific capacitance indicates that adding MWCNTs enhances the conducting pathway, which facilitates the overall charge transport process. The GCD cycles also support the cycle stability of the fabricated hybrid composite electrode (inset of Figure 10c). The capacitance retention was around 56% after 1000 cycles at a 2 A/g mass-specific current and the Coulombic efficiency was preserved by almost 100%, which can be attributed to the high electrical conductivity of the MWCNTs (Aruchamy et al. 2020).

Another advantage of using metal oxides is that they are low-cost materials with moderate capacitance. Therefore, the hybrid structure of metal oxide and MWCNT has gained increased attention. Combustion synthesis using an electric field is a facile method to fabricate the hybrid composite electrodes. As shown in Figure 10g, Shin et al. transformed a precursor solution of $Mn(NO_3)_2$/MWCNT/nitrocellulose into a $MnO_{2-x}$/MWCNT hybrid through sol-gel-driven combustion waves. Then, the activable hybrids ($MnO_{2-x}$/MWCNT) were transformed into supercapacitor electrodes ($MnO_2$/MWCNT) through electrochemical activation with $Na_2SO_4$ electrolyte. This electrochemical activation included 2000 charge/discharge cycles at a scan rate of 100 mV/s and produced electrodes with high porosity. As shown in Figures 10e & 10f, the fabricated hybrids exhibited an increase in capacitance of 42.5% during the first 100 cycles. After a total of 2000 charge/discharge cycles, highly stable capacitance retention (98.3%) was obtained. Shin et al. highlighted the oxidizing and anodizing of $MnO_{2-x}$ into $MnO_2$, which is caused by the electrochemical transition of the constituents. An increase in the porosity of the manganese oxide through electrochemical activation increases the active surface area and consequently enhances capacitance. The rectangular shape of the CV curves reveals the electrical conductivity of the hybrid electrodes. At the same time, the pair of redox peaks indicate the pseudocapacitive behavior of the electrodes (Figure 10d). Finally, the specific capacitance of the $MnO_2$/MWCNT was 169.5 F/g at a scan rate of 100 mV/s, demonstrating the successful production of hybrid electrodes with a high surface area and high stability (Shin et al. 2019).

### *Conducting polymer/MWCNT-based supercapacitor electrodes*

Conducting polymers are other candidate materials for supercapacitors, owing to their high electrical conductivity and pseudocapacitive behaviors. Common examples of conducting polymers include poly(3,4-ethylenedioxythiophene), polypyrrole, and polyaniline. Compared to the aforementioned metal oxides, conducting polymers have a larger specific capacitance. However, due to the repeated insertion and deinsertion of ions during charge/discharge cycles, conducting polymers show poor mechanical stability. Therefore, the addition of mechanically robust MWCNTs can overcome the disadvantages of conducting polymers. Moreover, metal oxides and conducting polymers are often used as anodes, whereas carbon materials are suitable as cathodes. The hybrid composite of a conducting polymer and MWCNT can be applied to both the positive and negative electrodes in supercapacitors. Furthermore, the low-cost advantage of both MWCNTs and conducting polymers makes them more versatile for application in diverse fields.

In supercapacitor applications, p-type polymers like poly(3,4-ethylenedioxythiophene), polypyrrole, and polyaniline are often used as electrodes because of their outstanding charge and storage characteristics. Thus, many reports on the use of p-type polymers for supercapacitors are available. However, donor-acceptor polymers such as P(NDI2OD-T2), also known as Polyera ActivInk N2200, need further research and performance improvement. The intrinsic redox properties of donor-acceptor polymers make them pseudocapacitive. In addition, they show high stability over long cycles and can withstand high-voltage windows. The ability to withstand high-voltage windows makes the use of organic electrolytes possible, which in turn can solve the low-voltage stability problems shown by conventional aqueous electrolytes. When the conjugated polymers are combined with MWCNTs, the $\pi$–$\pi$ interactions between the polymers and MWCNTs can also help prevent the aggregation of CNTs. Thus, the fabricated composite electrodes will have an ordered porous structure, facilitating the access of the electrolyte to the electrode. Wavhal et al. fabricated a high-voltage non-aqueous hybrid
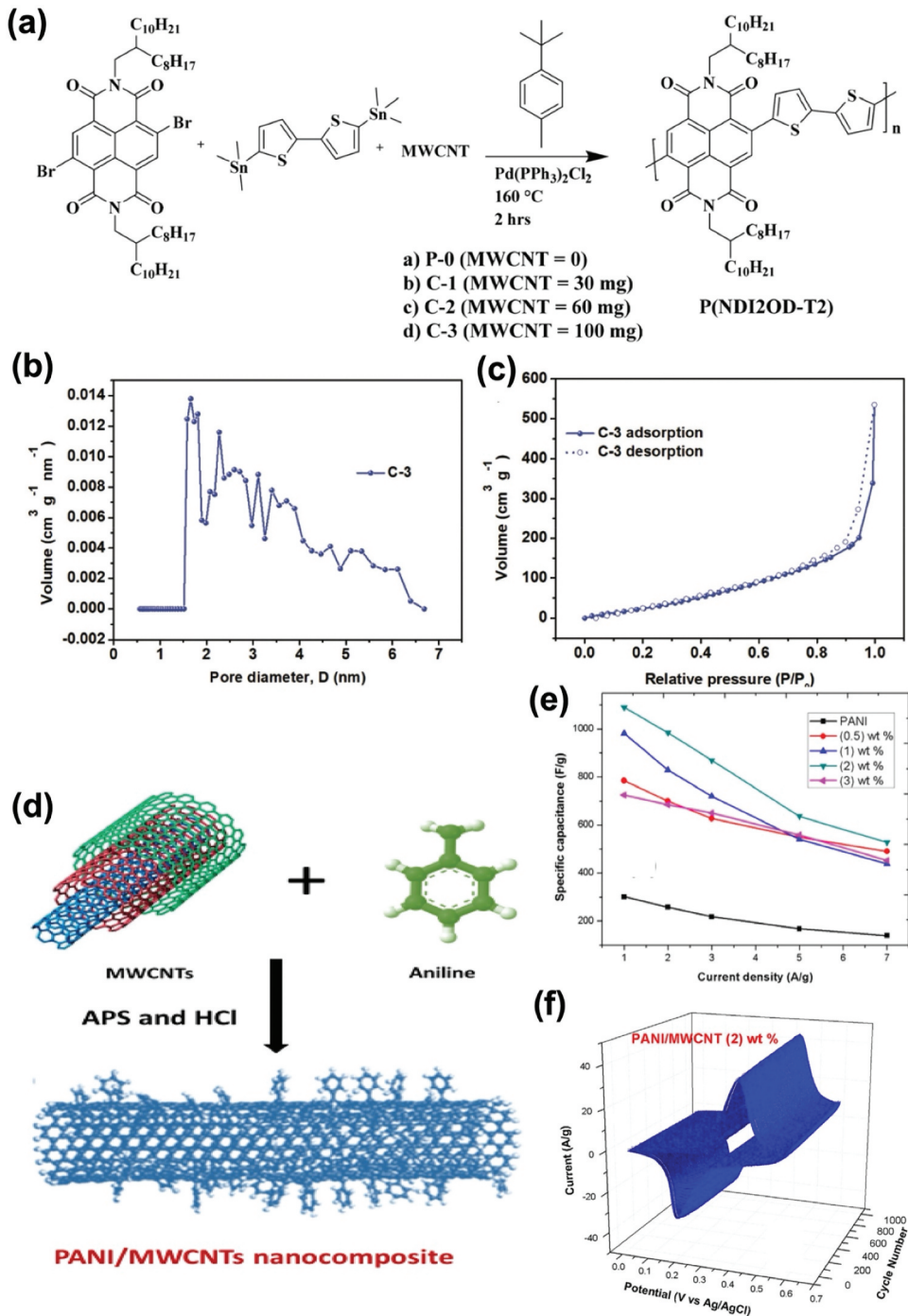
**Figure 11.** (a) Schematic diagram of the synthesis of a P(NDI2OD-T2) polymer and its incorporation into MWCNTs (Wavhal et al. 2021). (b) Pore size distribution profile and (c) nitrogen adsorption/desorption isotherm of the C-3 sample (Wavhal et al. 2021). (d) Schematic diagram of in situ PANI polymerization onto MWCNTs. (e) GCD curves of the specific capacitance of PANI/MWCNTs nanocomposites with different ratios of MWCNTs. (f) 3D CV curves of Ni foam with 2 wt.% PANI/MWCNTs (Awata et al. 2020). Reproduced with permission from (Awata et al. 2020; Wavhal et al. 2021).

supercapacitor in $LiClO_4$/propylene carbonate electrolyte based on the N2200 polymer with MWCNTs by *in situ* polymerization (Figure 11a). The modified version of the Stille polymerization was conducted and resulted in a high yield of high molecular weight polymers. The specific surface areas of the three samples (MWCNTs, N2200 polymer, and N2200 polymer/MWCNTs) were analyzed using the Brunauer-Emmett-Teller (BET) model. In Figures 11b, and c, the BET results showed 200.7, 81.1, and 224.8 $m^2 g^{-1}$, respectively, suggesting that the addition of MWCNTs increased the surface area. Figure 11b shows the pore size distribution profile of the N2200 polymer/MWCNT composite electrodes. Various pore diameters were observed in the sample, indicating that MWCNTs show both microporous and mesoporous morphologies. The mesoporous structure can improve the infiltration of the electrolyte into the electrodes. Moreover, the incorporation of MWCNTs also facilitated electron transport in the polymer. The CV and GCD curves both exhibited prominent redox peaks, indicating an increased charge storage ability. The capacitance retention value of 60% after 100 cycles at a current rate of 2.0 $Ag^{-1}$ demonstrated the cycling stability of the fabricated N2200 polymer/ MWCNT electrodes (Wavhal et al. 2021).

Awata et al. developed a camphor sulfonic acid-doped polyaniline (PANI)/MWCNT nanocomposite for supercapacitor applications. The nanocomposite was fabricated using a similar method as those used for donor-acceptor polymers, namely, *in situ* chemical oxidation polymerization (Figure 11d). Electrochemical analysis with the fabricated supercapacitor in 1 M $H_2SO_4$ solution revealed that the CV area of the PANI/MWCNT nanocomposite was larger than that of pure PANI. Moreover, the specific capacitance and energy density were also improved, owing to the strong $\pi-\pi$ interactions with the polymers and MWCNTs (Figure 11e). This in turn improved the interfacial contact between PANI and the electrolyte and minimized the charge transfer resistance. In addition, by incorporating MWCNTs, conductive networks with a highly ordered interface layer were produced, which facilitated both the ion transportation and redox reaction. Specific capacitance retention of 100% was obtained after 1000 cycles, demonstrating that the incorporation of MWCNTs results in increased reversibility (Awata et al. 2020)(Figure 11f).

### Hydrogel/mwcnt-based supercapacitor electrodes

A hydrogel has a three-dimensional porous architecture because of its hydrophilic polymer chains. Among the various types of hydrogels, conducting polymer hydrogels exhibit the advantages of both conducting polymers and hydrogels, having superior electrical characteristics as well as electrochemical properties. Polymer hydrogels are considered promising materials for supercapacitors due to their morphologies that allow fast ion and electron diffusion. PANI hydrogels could be applied in supercapacitors because of their large pseudocapacitance, flexibility, and moderate conductivity. The biggest advantage of using PANI hydrogels is that they do not require binders, thus resulting in good adhesion between the current collector and electrode. The problems of using binders include the degradation of the specific capacitance of the supercapacitor and the formation of residues However, PANI hydrogels experience volumetric changes and mechanical degradation during charge/discharge processes, which lowers their cyclic stability. Sardana et al. proposed the amalgamation of PANI hydrogels with MWCNTs to overcome this problem, considering that MWCNTs show mechanical robustness and stability. Moreover, the well-dispersed MWCNTs have a large surface contact area, facilitating the electron conduction pathway. As shown in Figure 12a, the PANI/MWCNT composite hydrogel was fabricated via *in situ* oxidative polymerization of aniline, phytic acid, and carbon cloth. The XRD plots (Figure 12b) show similar patterns of the diffraction peak for both the PANI/MWCNT composite hydrogel and the PANI hydrogel. This result suggests that the addition of MWCNT did not alter the crystallinity of the PANI hydrogel. The synthesized PANI/MWCNT composite hydrogel exhibited 246.67 F/g at a scan rate of 20 mV/s. However, the maximum specific capacitance value decreased to 208.35 F/g at a 100 mV/s scan rate because the electrolyte ions had a shorter time to diffuse in the surface area of the electrode at a higher scan rate (Figure 12c). The cyclic stability of the PANI/MWCNT composite hydrogel electrode with 1 M $H_2SO_4$ electrolyte was analyzed by applying the GCD technique. Figure 12d depicts the cyclic stability of the electrodes during 5000 charge/
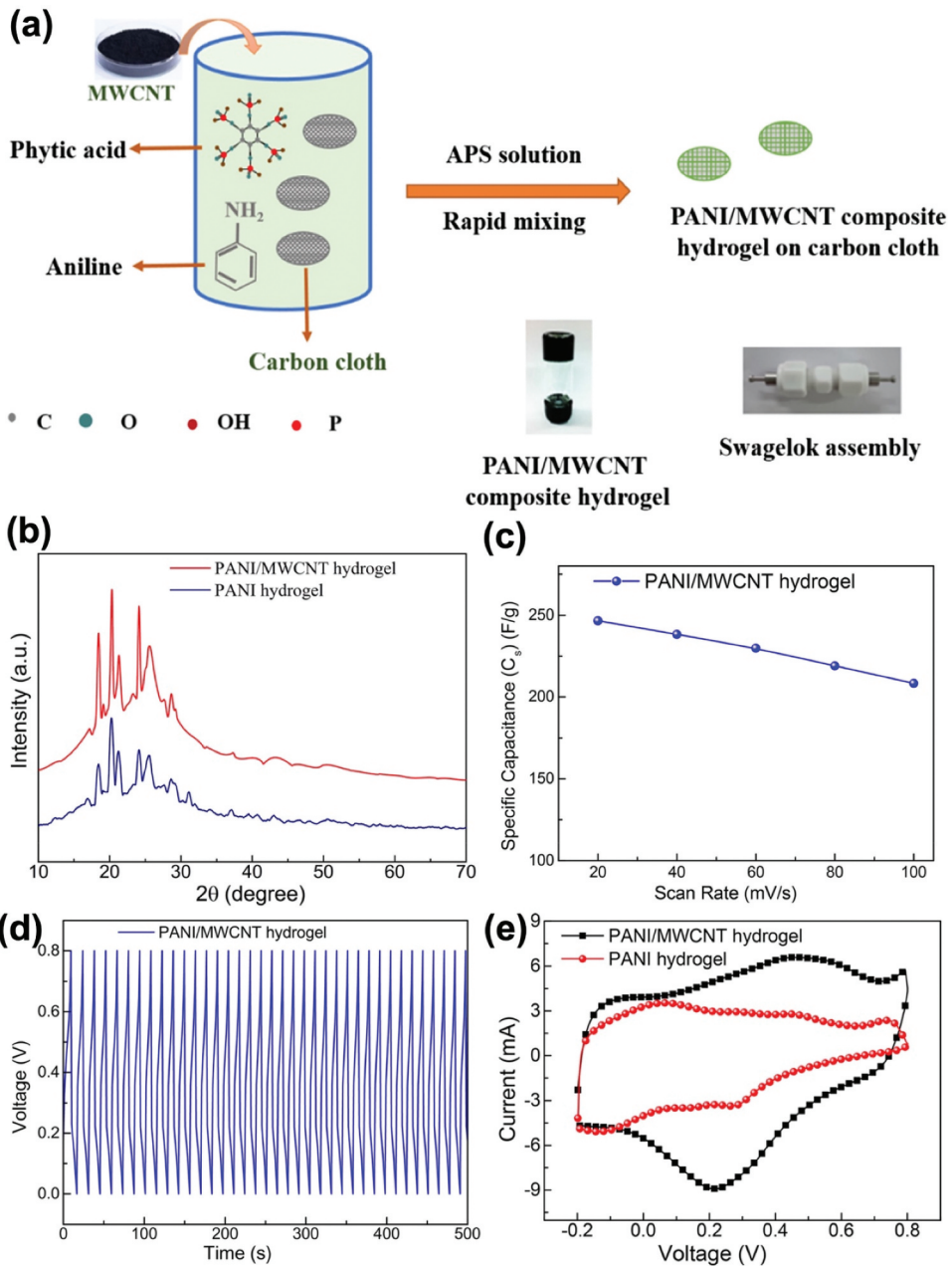
**Figure 12.** (a) Schematic diagram of the fabrication of the PANI/MWCNT composite hydrogel (inset: a snapshot of the PANI/MWCNT composite hydrogel in a glass ampoule and Swagelok assembly for electrochemical measurements). (b) XRD plots of PANI/MWCNT and pure PANI hydrogels. (c) Specific capacitance of the PANI/MWCNT hydrogel at various scan rates. (d) Charge/discharge plots of the PANI/MWCNT hydrogel at a current density of 10 A/g for several cycles. (e) CV plots of PANI/MWCNT and pure PANI hydrogels. Reproduced with permission from (Silki et al. 2022).

discharge cycles at a current density of 10 A/g. The CV plots for both the PANI/MWCNT composite hydrogel and the PANI hydrogel exhibit redox peaks, which indicate pseudocapacitive characteristics (Figure 12e). The specific capacitance value of the PANI/MWCNT composite hydrogel was 277.59 F/g, while that of the PANI hydrogel was 142.24 F/g at a current density of 0.25 A/g. The increase in the specific capacitance demonstrates the well-designed structure of the two components. The EDLC

storage in MWCNTs and pseudocapacitance of PANI exhibited synergistic effects on the performance of the flexible supercapacitor (Silki et al. 2022).

Another advantage of hydrogel-based electrodes is that by adding functional materials or functionalization, desired functions such as self-healing, stretchability, and sensitivity to external stimuli can be obtained. Depending on the functions achieved, hydrogels can be applied to various fields from energy storage devices to sensors. For supercapacitor applications, the hydrogel-based electrode materials should enhance their ionic and electronic conductivity, electrolyte permeability, and other electrochemical performance. Liu et al. developed a gelatin/MWCNT-polypyrrole (PPy) gel with wrinkled structures that exhibited high stretchability and self-healing properties in addition to electrochemical characteristics. The composite hydrogel electrode was synthesized by a simple soaking-heating-template coating-resoaking (SHTR) method as shown in Figure 13a. The incorporation of MWCNTs to the gelatin not only increased the electrical conductivity but also the mechanical strength, and thus enhanced the electrochemical and mechanical properties of the supercapacitor. This was demonstrated by the loading-unloading tests of the fabricated H-gel/AS-MWCNT-PPy-AS gel, which exhibited less residual strain and moderate fatigue resistance compared to the gel without MWCNTs. The cyclic tensile behavior of the H-gel/AS-MWCNT-PPy-AS gel at a strain of 25% after 500 cycles showed low hysteresis and recovery, suggesting self-healing properties. Moreover, the unique structural design with wrinkles increased the surface area of the interface between the electrode
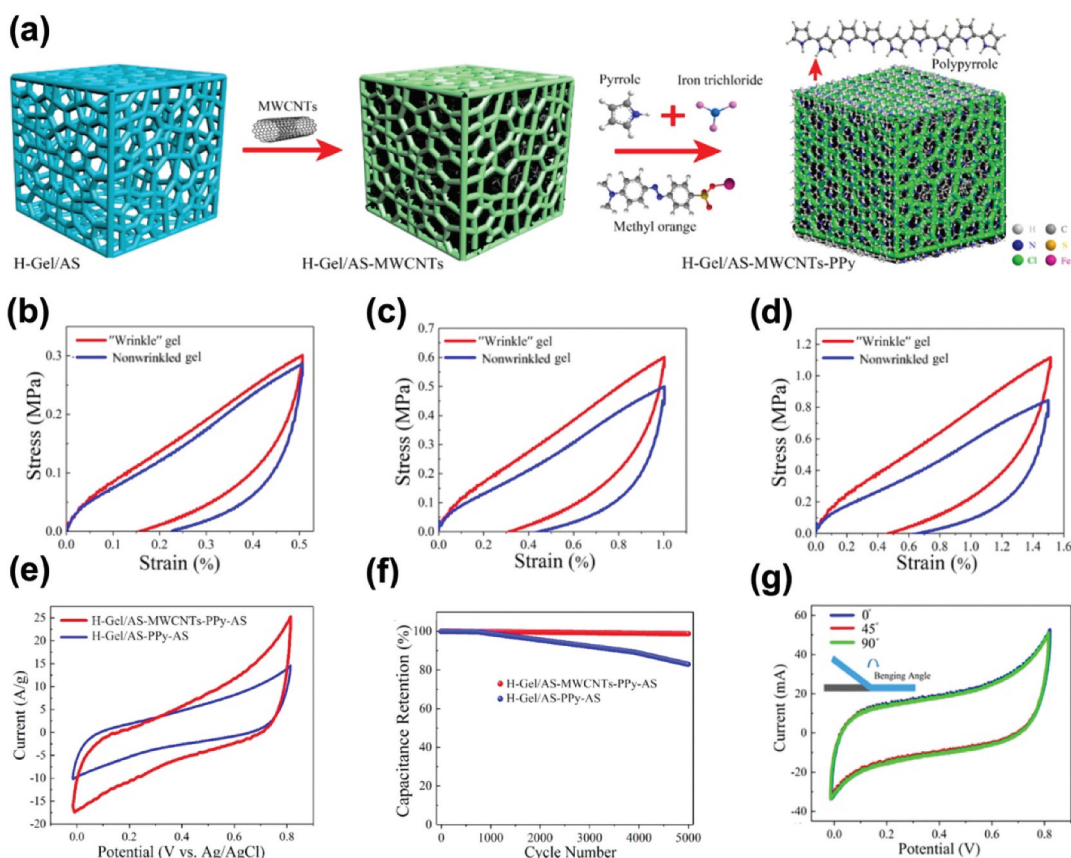


**Figure 13.** (a) Schematic diagram of the production of a gelatin hydrogel electrolyte. Cycle tensile loading-unloading curves of the wrinkled and nonwrinkled gels at (b) 50% strain, (c) 100% strain, and (d) 150% strain. (e) CV curves at a scan rate of 100 mV/s. (f) Capacitance retention of H-gel/AS-PPy-AS and H-gel/AS-MWCNTs-PPy-AS gels. (g) CV curves of the fabricated supercapacitor under different bending conditions at a scan rate of 100 mV/s. Reproduced with permission from (Bu et al. 2021).

**Table 1.** Summary of previous studies of CNT-based supercapacitors.

| Electrodes | | Electrolytes | Specific Capacitance | Current Density | Capacitance Retention | Cycle number | Ref. |
|---|---|---|---|---|---|---|---|
| SWCNT | Polymer | TBN-based Conjugated Microporous Polymers (CMP) | KOH | 430 Fg⁻¹ | 0.5 Ag⁻¹ | 99.18% | 2000 | (Samy et al. 2021) |
| | Polymer | Poly(3-hexylthiophene) (P3HT) | LiClO₄ | 245.8 Fg⁻¹ | 0.5 Ag⁻¹ | 80.5% | 1000 | (Shokry et al. 2022) |
| | Polymer | PEDOT-MeOH | H₂SO₄ | 114.3 mFcm⁻² | 5 mVs⁻¹ | 80% | 5000 | (Zhang et al. 2020) |
| | Polymer | Poly(3-oligo(ethylene oxide)thiophene (PD2ET) | PVA/KCl | 399 Fg⁻¹ | 1 Ag⁻¹ | 91% | 8000 | (Zhou et al. 2019) |
| | Hydrogel | PEDOT:PSS Hydrogel/Composite Cotton | Poly(acrylamide)/Na-alginate hydrogel | 212.16 Fg⁻¹ | 50 mVs⁻¹ | N/A | N/A | (Badawi, Batoo et al. 2023) |
| | Hydrogel | MoS₂ Nanosheet/Cellulose Nanofibril Hybrid Aerogel | PVA/H2SO4 gel | 30.34 Fg⁻¹ | 0.01 Ag⁻¹ | 91.01% | 10000 | (Chang et al. 2022) |
| DWCNT | Carbon Material | Xanthan gum-derived Activated Carbon (AC) | H₂SO₄ | 141.5 Fg⁻¹ | 100 mVs⁻¹ | N/A | N/A | (Kang et al. 2020) |
| | Carbon Material | Nitrogen-doped (NG) Graphene Nanosheet | H₂SO₄ | 563 Fg⁻¹ | 50 Ag⁻¹ | 94.35% | 5000 | (Muangrat et al. 2021) |
| | Metal Oxide | Metal Organic Frameworks (MOFs) | PVA-DMSO gel | 151.1 Fg⁻¹ | 1 Ag⁻¹ | 87.4% | 500 | (Na et al. 2022) |
| MWCNT | Transition Metal Oxide | Sol-gel driven MnO₂ | Na₂SO₄ | 259.6 Fg⁻¹ | 100 mVs⁻¹ | 91% | 10000 | (Shin et al. 2019) |
| | Transition Metal Oxide | Spinel ZnMn₂O₄ Nanoparticles | Na₂SO₄ | 103 Fg⁻¹ | 1 mVs⁻¹ | 85% | 1000 | (Aruchamy et al. 2020) |
| | Polymer | N2200 Polymer | LiClO₄/propylene carbonate | 80 mAhg⁻¹ | 2 Ag⁻¹ | 80% | 2500 | (Wavhal et al. 2021) |
| | Polymer | Camphor Sulfonic Acid doped PANI | H₂SO₄ | 1183 Fg⁻¹ | 1 Ag⁻¹ | 87% | 1000 | (Awata et al. 2020) |
| | Hydrogel | PANI composite Hydrogel | H₂SO₄ | 277.59 Fg⁻¹ | 0.25 Ag⁻¹ | N/A | 5000 | (Silki et al. 2022) |
| | Hydrogel | H-Gel/AS-MWCNTs-PPy gel | N/A | 112.5 Fg⁻¹ | 0.5 Ag⁻¹ | 98.1% | 5000 | (Bu et al. 2021) |

and electrolyte, improving the capacitance behavior. As shown in Figure 13b–d small hysteresis was maintained under 50, 100, and 150% strain, suggesting excellent mechanical stability. The large CV curve area in Figure 13e indicates a high-rate performance. The calculated specific capacitance was 112.5 F/g for the H-gel/AS-MWCNT-PPy-AS gel and 56.25 F/g for gels without MWCNTs. The 5000 GCD cycles in Figure 13f demonstrated outstanding capacity and Coulombic retention. Liu et al. claimed that the incorporation of MWCNTs improved the electrical conductivity and surface area, which in turn helped the electron transport during the charge/discharge processes. Figure 13g shows the unchanged curves for CV under bending conditions of 45° and 90°, demonstrating the potential of this material to be applied to flexible supercapacitors (Bu et al. 2021).

## Conclusion

In this review, recent technological trends of CNT-based flexible supercapacitor electrodes were discussed according to the structural types of CNTs. The unique structural properties, flexibility, mechanical robustness, and electrochemical properties of CNTs make them promising materials for supercapacitor applications. Many reports have been published regarding the use of CNTs as electrode materials and have mainly focused on design strategies or fabrication techniques. However, to our knowledge, a review of CNT-based supercapacitor electrodes classified according to the CNT structure (SWCNT, DWCNT, and MWCNT) is unavailable. A comparison of the electrochemical properties including specific capacitance and capacitance retention of the CNT-based electrodes is provided in Table 1. Specific capacitance values ranging from 150 to 250 $Fg^{-1}$ and cyclic stability for more than 1000 cycles demonstrated the potential of the electrodes to be applied to flexible supercapacitor devices. SWCNT-based flexible supercapacitors exhibited relatively high specific capacitance and outstanding cycling stability compared to DWCNT or MWCNT based flexible supercapacitors.

Current research trend tends to incorporate various composite materials such as polymers, hydrogels, and metal oxides with CNTs to optimize the inherent merits of the CNTs. Despite the recent progress in CNT-based flexible supercapacitors, there are still challenges that need to be solved for their practical applications. First, composite materials including polymers and metal oxides are often utilized to improve the intrinsic properties of CNTs by inducing higher energy densities of the supercapacitors. However, power densities and long-term durability may be degraded via those addition of pseudo-capacitive materials. Thus, improvements are necessary for increasing the energy densities while preserving the power capabilities and cycle durability (Olabi et al. 2023). Second, mechanical behaviors of CNT-based flexible supercapacitors should be improved further to allow practical applications to the wearable electronic industries. Bulky and heavy supercapacitors limit portable and wearable applications, therefore ways to decrease the vol% of CNTs and other composite materials with preserving the electrochemical performances should be studied further. Additionally, the mechanical properties of flexible supercapacitors should match that of human tissues to be applied as wearable electronic devices (Jeerapan and Nicolás 2019). Focusing on distributing CNTs in other composite materials can also be the fundamental solutions for enhancing the performance of CNT-based flexible supercapacitors as well (Nurazzi et al. 2021). Finally, challenges regarding the mass production of CNT-based flexible supercapacitors should also be overcome. The fabricating process with high throughput synthesis should be held in large scale, allowing commercial application.

## Acknowledgements

## Disclosure statement

No potential conflict of interest was reported by the authors.

## Funding

## Highlights

- Carbon nanotubes (CNTs)-based flexible supercapacitors (FSCs) were classified according to the structural types of CNTs and the materials incorporated.
- The overall electrochemical properties and mechanical stability of the reported FSC electrodes based on SWCNT, DWCNT, and MWCNT are compared.
- Technological trends and future research direction of CNT-based flexible supercapacitors are discussed.

## References

Agrawal, P. M., B. S. Sudalayandi, L. M. Raff, and R. Komanduri. 2006. A comparison of different methods of Young's modulus determination for single-wall carbon nanotubes (SWCNT) using molecular dynamics (MD) simulations. *Computational Materials Science* 38 (2):271–81. doi:10.1016/j.commatsci.2006.02.011.

An, K. H., K. K. Jeon, J. K. Heo, S. C. Lim, D. J. Bae, and Y. H. Lee. 2002. High-Capacitance supercapacitor using a nanocomposite electrode of single-walled carbon nanotube and polypyrrole. *Journal of the Electrochemical Society* 149 (8):A1058. doi:10.1149/1.1491235.

Ansari, R., M. Mirnezhad, and S. Sahmani. 2013. An accurate molecular mechanics model for computation of size-dependent elastic properties of armchair and zigzag single-walled carbon nanotubes. *Meccanica* 48 (6):1355–67. doi:10.1007/s11012-012-9671-x.

Aruchamy, K., R. Nagaraj, H. M. Manohara, M. R. Nidhi, D. Mondal, D. Ghosh, and S. K. Nataraj. 2020. One-step green route synthesis of spinel ZnMn2O4 nanoparticles decorated on MWCNTs as a novel electrode material for supercapacitor. *Materials Science and Engineering: B* 252:114481. doi:10.1016/j.mseb.2019.114481.

Awata, R., M. Shehab, A. El Tahan, M. Soliman, and S. Ebrahim. 2020. High performance supercapacitor based on camphor sulfonic acid doped polyaniline/multiwall carbon nanotubes nanocomposite. *Electrochimica acta* 347:136229. doi:10.1016/j.electacta.2020.136229.

Aziz, S. B., J. M. Hadi, E. M. Dannoun, R. T. Abdulwahid, S. R. Saeed, A. Shahab Marf, W. O. Karim, and M. F. Kadir. 2020. The study of plasticized amorphous biopolymer blend electrolytes based on polyvinyl alcohol (PVA): Chitosan with high ion conductivity for energy storage electrical double-layer capacitors (EDLC) device application. *Polymers* 12 (9):1938. doi:10.3390/polym12091938.

Badawi, N. M., M. Bhatia, S. Ramesh, K. Ramesh, M. Kuniyil, M. R. Shaik, M. Khan, B. Shaik, and S. F. Adil. 2023. Self-healing, flexible and smart 3d hydrogel electrolytes based on alginate/PEDOT: PSS for supercapacitor applications. *Polymers (Basel)* 15:3. doi:10.3390/polym15030571.

Badawi, N. M., S. R. Khalid Mujasam Batoo, S. Ramesh, K. Ramesh, and A. Imran. 2023. Swcnts/PEDOT: PSS Coated Cotton for Wearable Clothes and Supercapacitor Applications. *Sustainability* 15 (1):889.

Basirjafari, S., S. Esmaielzadeh Khadem, and R. Malekfar. 2013. Determination of the inner diameter of a double-walled carbon nanotube from its Raman spectra. *Journal of Applied Physics* 113 (6):064304. doi:10.1063/1.4790162.

Benguediab, S., A. Tounsi, M. Zidour, and A. Semmah. 2014. Chirality and scale effects on mechanical buckling properties of zigzag double-walled carbon nanotubes. *Composites Part B: Engineering* 57:21–24. doi:10.1016/j.compositesb.2013.08.020.

Boumia, L., M. Zidour, A. Benzair, and A. Tounsi. 2014. A Timoshenko beam model for vibration analysis of chiral single-walled carbon nanotubes. *Physica. E, Low-Dimensional Systems & Nanostructures* 59:186–91. doi:10.1016/j.physe.2014.01.020.

Bu, Y., T. Shen, W. Yang, S. Yang, Y. Zhao, H. Liu, Y. Zheng, C. Liu, and C. Shen. 2021. Ultrasensitive strain sensor based on superhydrophobic microcracked conductive Ti3C2Tx MXene/paper for human-motion monitoring and E-skin. *Science Bulletin* 66 (18):1849–57. doi:10.1016/j.scib.2021.04.041.

Celzard, A., F. Collas, J. F. Marêché, G. Furdin, and I. Rey. 2002. Porous electrodes-based double-layer supercapacitors: Pore structure versus series resistance. *Journal of Power Sources* 108 (1):153–62. doi:10.1016/S0378-7753(02)00030-7.

Chang, H., L. Zhang, S. Lyu, and S. Wang. 2022. Flexible and freestanding MoS2 nanosheet/carbon nanotube/cellulose nanofibril hybrid aerogel film for high-performance all-solid-state supercapacitors. *ACS Omega* 7 (16):14390–99. doi:10.1021/acsomega.2c01815.

Charoenpakdee, J., O. Suntijitrungruang, and S. Boonchui. 2020. Chirality effects on an electron transport in single-walled carbon nanotube. *Scientific Reports* 10 (1):18949. doi:10.1038/s41598-020-76047-9.

Chen, T., and L. Dai. 2014. Flexible supercapacitors based on carbon nanomaterials. *Journal of Materials Chemistry A* 2 (28):10756–75. doi:10.1039/c4ta00567h.

Chen, D., K. Jiang, T. Huang, and G. Shen. 2020. Recent advances in fiber supercapacitors: Materials, device configurations, and applications. *Advanced Materials* 32 (5):1901806. doi:10.1002/adma.201901806.

Chen, R., J. Liang, J. Lee, V. P. Georgiev, R. Ramos, H. Okuno, D. Kalita, Y. Cheng, L. Zhang, R. R. Pandey, et al. 2018a. Variability study of MWCNT local interconnects considering defects and contact resistances—Part I: Pristine MWCNT. *IEEE Transactions on Electron Devices* 65 (11):4955–62. doi:10.1109/TED.2018.2868421.

Chen, R., J. Liang, J. Lee, V. P. Georgiev, R. Ramos, H. Okuno, D. Kalita, Y. Cheng, L. Zhang, R. R. Pandey, et al. 2018b. Variability study of MWCNT local interconnects considering defects and contact resistances—Part II: Impact of charge transfer doping. *IEEE Transactions on Electron Devices* 65 (11):4963–70. doi:10.1109/TED.2018.2868424.

Chen, H., S. Zeng, M. Chen, Y. Zhang, and Q. Li. 2015. Fabrication and functionalization of carbon nanotube films for high-performance flexible supercapacitors. *Carbon* 92:271–96. doi:10.1016/j.carbon.2015.04.010.

Cherusseri, J., D. Pandey, K. Sambath Kumar, J. Thomas, and L. Zhai. 2020. Flexible supercapacitor electrodes using metal–organic frameworks. *Nanoscale* 12 (34):17649–62. doi:10.1039/D0NR03549A.

Choi, C., D. S. Ashby, D. M. Butts, R. H. DeBlock, Q. Wei, J. Lau, and B. Dunn. 2020. Achieving high energy density and high power density with pseudocapacitive materials. *Nature Reviews Materials* 5 (1):5–19. doi:10.1038/s41578-019-0142-z.

Ci, L., Z. Rao, Z. Zhou, D. Tang, X. Yan, Y. Liang, D. Liu, H. Yuan, W. Zhou, G. Wang, et al. 2002. Double wall carbon nanotubes promoted by sulfur in a floating iron catalyst CVD system. *Chemical Physics Letters* 359 (1–2):63–67. doi:10.1016/S0009-2614(02)00600-0.

Curtin, W. A., and B. W. Sheldon. 2004. CNT-reinforced ceramics and metals. *Materials Today* 7 (11):44–49. doi:10.1016/S1369-7021(04)00508-5.

Dai, H. 2002. Carbon nanotubes: Synthesis, integration, and properties. *Accounts of Chemical Research* 35 (12):1035–44. doi:10.1021/ar0101640.

Da Silva, L. M., R. Cesar, C. M. Moreira, J. H. Santos, L. G. De Souza, B. M. Pires, R. Vicentini, W. Nunes, and H. Zanin. 2020. Reviewing the fundamentals of supercapacitors and the difficulties involving the analysis of the electrochemical findings obtained for porous electrode materials. *Energy Storage Materials* 27:555–90. doi:10.1016/j.ensm.2019.12.015.

Datta, S., S. Wang, C. Tilmaciu, E. Flahaut, L. Marty, M. Grifoni, and W. Wernsdorfer. 2011. Electronic transport properties of double-wall carbon nanotubes. *Physical Review B* 84 (3):035408. doi:10.1103/PhysRevB.84.035408.

Di Bartolomeo, A., M. Rinzan, A. K. Boyd, Y. Yang, L. Guadagno, F. Giubileo, and P. Barbara. 2010. Electrical properties and memory effects of field-effect transistors from networks of single-and double-walled carbon nanotubes. *Nanotechnology* 21 (11):115204. doi:10.1088/0957-4484/21/11/115204.

Doh, J., S.I. Park, Q. Yang, and N. Raghavan. 2019. The effect of carbon nanotube chirality on the electrical conductivity of polymer nanocomposites considering tunneling resistance. *Nanotechnology* 30 (46):465701. doi:10.1088/1361-6528/ab3b79.

Domagała, K., M. Borlaf, J. Traber, D. Kata, and T. Graule. 2019. Purification and functionalisation of multi-walled carbon nanotubes. *Materials Letters* 253:272–75. doi:10.1016/j.matlet.2019.06.085.

Eatemadi, A., H. Daraee, H. Karimkhanloo, M. Kouhi, N. Zarghami, A. Akbarzadeh, M. Abasi, Y. Hanifehpour, and S. Woo Joo. 2014. Carbon nanotubes: Properties, synthesis, purification, and medical applications. *Nanoscale Research Letters* 9 (1):1–13. doi:10.1186/1556-276X-9-393.

Esawi, A. M. K., K. Morsi, A. Sayed, M. Taher, and S. Lanka. 2011. The influence of carbon nanotube (CNT) morphology and diameter on the processing and properties of CNT-reinforced aluminium composites. *Composites Part A, Applied Science and Manufacturing* 42 (3):234–43. doi:10.1016/j.compositesa.2010.11.008.

Faraji, S., and F. Nasir Ani. 2015. The development supercapacitor from activated carbon by electroless plating—A review. *Renewable and Sustainable Energy Reviews* 42:823–34. doi:10.1016/j.rser.2014.10.068.

Faria, B., N. Silvestre, and J. N. Canongia Lopes. 2013. Tension–twisting dependent kinematics of chiral CNTs. *Composites Science and Technology* 74:211–20. doi:10.1016/j.compscitech.2012.11.010.

Gao, S., K. Wang, Z. Du, Y. Wang, A. Yuan, W. Lu, and L. Chen. 2015. High power density electric double-layer capacitor based on a porous multi-walled carbon nanotube microsphere as a local electrolyte micro-reservoir. *Carbon* 92:254–61. doi:10.1016/j.carbon.2015.04.034.

Gaviria Rojas, W. A., and M. C. Hersam. 2020. Chirality-enriched carbon nanotubes for next-generation computing. *Advanced Materials* 32 (41):1905654. doi:10.1002/adma.201905654.

Gnanasekaran, K., T. Heijmans, S. Van Bennekom, H. Woldhuis, S. Wijnia, G. De with, and H. Friedrich. 2017. 3D printing of CNT-and graphene-based conductive polymer nanocomposites by fused deposition modeling. *Applied Materials Today* 9:21–28. doi:10.1016/j.apmt.2017.04.003.

Gong, X., Q. Yang, C. Zhi, and P. See Lee. 2021. Stretchable energy storage devices: From materials and structural design to device assembly. *Advanced Energy Materials* 11 (15):2003308. doi:10.1002/aenm.202003308.

Gregg, A., M. F. De Volder, and J. J. Baumberg. 2022. Light-actuated anisotropic microactuators from CNT/hydrogel nanocomposites. *Advanced Optical Materials* 10 (13):2200180. doi:10.1002/adom.202200180.

Guillet, J.F., Z. Valdez-Nava, M. Golzio, and E. Flahaut. 2019. Electrical properties of double-wall carbon nanotubes nanocomposite hydrogels. *Carbon* 146:542–48. doi:10.1016/j.carbon.2019.01.090.

Han, L., Q. Song, J. Sun, K. Li, and Y. Lu. 2020. The role of CNT in improving the mechanical strength retention rate of C/C composites during heat treatment. *Composites Part B: Engineering* 187:107856. doi:10.1016/j.compositesb.2020.107856.

Hároz, E. H., J. G. Duque, X. Tu, M. Zheng, A. R. Walker, R. H. Hauge, S. K. Doorn, and J. Kono. 2013. Fundamental optical processes in armchair carbon nanotubes. *Nanoscale* 5 (4):1411–39. doi:10.1039/c2nr32769d.

Hillier, N., S. Yong, and S. Beeby. 2020. The good, the bad and the porous: A review of carbonaceous materials for flexible supercapacitor applications. *Energy Reports* 6:148–56. doi:10.1016/j.egyr.2020.03.019.

Hou, P. -X., C. Liu, and H. -M. Cheng. 2008. Purification of carbon nanotubes. *Carbon* 46 (15):2003–25. doi:10.1016/j.carbon.2008.09.009.

Iijima, S. 1991. Helical microtubules of graphitic carbon. *Nature* 354 (6348):56–58. doi:10.1038/354056a0.

Ike, I. S., I. Sigalas, and S. Iyuke. 2016. Understanding performance limitation and suppression of leakage current or self-discharge in electrochemical capacitors: A review. *Physical Chemistry Chemical Physics* 18 (2):661–80. doi:10.1039/C5CP05459A.

Imazu, N., T. Fujigaya, and N. Nakashima. 2015. Fabrication of highly transparent, thermally stable, and scalable conductive films from double-walled carbon nanotubes. *Bulletin of the Chemical Society of Japan* 88 (1):217–21. doi:10.1246/bcsj.20140277.

Ismail, A. F., P. S. Goh, J. C. Tee, S. M. Sanip, and M. Aziz. 2008. A REVIEW OF PURIFICATION TECHNIQUES FOR CARBON NANOTUBES. *Nano* 03 (03):127–43. doi:10.1142/S1793292008000927.

Jeerapan, I., and M. Nicolás. 2019. Challenges and opportunities of carbon nanomaterials for biofuel cells and super-capacitors: Personalized energy for futuristic self-sustainable devices. *C — Journal of Carbon Research* 5 (4):62. doi:10.3390/c5040062.

Jeon, I., J. Yoon, U. Kim, C. Lee, R. Xiang, A. Shawky, J. Xi, J. Byeon, H. Mo Lee, and M. Choi. 2019. High-performance solution-processed double-walled carbon nanotube transparent electrode for perovskite solar cells. *Advanced Energy Materials* 9 (27):1901204. doi:10.1002/aenm.201901204.

Jiang, Y., and J. Liu. 2019. Definitions of pseudocapacitive materials: A brief review. *ENERGY & ENVIRONMENTAL MATERIALS* 2 (1):30–37. doi:10.1002/eem2.12028.

Jia, F., C. Yu, K. Deng, and L. Zhang. 2007. Nanoporous metal (Cu, Ag, Au) films with high surface area: General fabrication and preliminary electrochemical performance. *The Journal of Physical Chemistry C* 111 (24):8424–31. doi:10.1021/jp071815y.

Joselevich, E. 2006. Twisting nanotubes: From torsion to chirality. *Chemphyschem: A European Journal of Chemical Physics and Physical Chemistry* 7 (7):1405–07. doi:10.1002/cphc.200600206.

Jung, S. I., S. H. Jo, H. S. Moon, J. M. Kim, D. -S. Zang, and C. J. Lee. 2007. Improved crystallinity of double-walled carbon nanotubes after a high-temperature thermal annealing and their enhanced field emission properties. *The Journal of Physical Chemistry C* 111 (11):4175–79. doi:10.1021/jp0676078.

Kang, C. -S., Y. -I. Ko, K. Fujisawa, T. Yokokawa, J. Hee Kim, J. Hun Han, J. -H. Wee, Y. Ahm Kim, H. Muramatsu, and T. Hayashi. 2020. Hybridized double-walled carbon nanotubes and activated carbon as free-standing electrode for flexible supercapacitor applications. *Carbon Letters* 30 (5):527–34. doi:10.1007/s42823-020-00122-4.

Kanoun, O., A. Bouhamed, R. Ramalingame, J. Roberto Bautista-Quijano, D. Rajendran, and A. Al-Hamry. 2021. Review on conductive polymer/CNTs nanocomposites based flexible and stretchable strain and pressure sensors. *Sensors* 21 (2):341. doi:10.3390/s21020341.

Kim, H., P. Matteini, and B. Hwang. 2022. Mini review of reliable fabrication of electrode under stretching for supercapacitor application. *Micromachines* 13 (9):1470. doi:10.3390/mi13091470.

Kim, G. M., I. W. Nam, H. Y. Beomjoo Yang, H.K. Lee, and S. Park. 2019. Carbon nanotube (CNT) incorporated cementitious composites for functional construction materials: The state of the art. *Composite Structures* 227:111244. doi:10.1016/j.compstruct.2019.111244.

Kim, D. -H., and J. A. Rogers. 2008. Stretchable electronics: Materials strategies and devices. *Advanced Materials* 20 (24):4887–92. doi:10.1002/adma.200801788.

Kim, H. -I., M. Wang, S. K. Lee, J. Kang, J. -D. Nam, L. Ci, and J. Suhr. 2017. Tensile properties of millimeter-long multi-walled carbon nanotubes. *Scientific Reports* 7 (1):1–7. doi:10.1038/s41598-017-10279-0.

Kim, G. M., B. J. Yang, K. J. Cho, E. M. Kim, and H.K. Lee. 2017. Influences of CNT dispersion and pore characteristics on the electrical performance of cementitious composites. *Composite Structures* 164:32–42. doi:10.1016/j.compstruct.2016.12.049.

Kim, Y. A., K. -S. Yang, H. Muramatsu, T. Hayashi, M. Endo, M. Terrones, and M. S. Dresselhaus. 2014. Double-walled carbon nanotubes: Synthesis, structural characterization, and application. *Carbon Letters* 15 (2):77–88. doi:10.5714/CL.2014.15.2.077.

Kobashi, K., H. Nishino, T. Yamada, D. N. Futaba, M. Yumura, and K. Hata. 2011. Epoxy composite sheets with a large interfacial area from a high surface area-supplying single-walled carbon nanotube scaffold filler. *Carbon* 49 (15):5090–98. doi:10.1016/j.carbon.2011.07.028.

Kociak, M., K. Suenaga, K. Hirahara, Y. Saito, T. Nakahira, and S. Iijima. 2002. Linking chiral indices and transport properties of double-walled carbon nanotubes. *Physical Review Letters* 89 (15):155501. doi:10.1103/PhysRevLett.89.155501.

Kwon, Y.K., and D. Tománek. 1998. Electronic and structural properties of multiwall carbon nanotubes. *Physical Review B* 58 (24):R16001. doi:10.1103/PhysRevB.58.R16001.

Lair, S. L., W. C. Herndon, and L. E. Murr. 2008. Stability comparison of simulated double-walled carbon nanotube structures. *Carbon* 46 (15):2083–95. doi:10.1016/j.carbon.2008.08.022.

Laurent, C., E. Flahaut, and A. Peigney. 2010. The weight and density of carbon nanotubes versus the number of walls and diameter. *Carbon* 48 (10):2994–96. doi:10.1016/j.carbon.2010.04.010.

Lee, S. H., E. Cho, S. Hee Jeon, and J. Ryoun Youn. 2007. Rheological and electrical properties of polypropylene composites containing functionalized multi-walled carbon nanotubes and compatibilizers. *Carbon* 45 (14):2810–22. doi:10.1016/j.carbon.2007.08.042.

Lee, H., G. Lee, J. Yun, K. Keum, S. Yeong Hong, C. Song, J. Wook Kim, J. Ho Lee, S. Y. Oh, and D. Sik Kim. 2019. Facile fabrication of a fully biodegradable and stretchable serpentine-shaped wire supercapacitor. *Chemical Engineering Journal* 366:62–71. doi:10.1016/j.cej.2019.02.076.

Lei, C., and C. Lekakou. 2010. Carbon-based nanocomposite EDLC supercapacitors*Advanced Materials, CNTs, Particles, Films and Composites. Nanotechnology* 1:176–79. *2010*.

Lian, F., J. P. Llinas, Z. Li, D. Estrada, and E. Pop. 2016. Thermal conductivity of chirality-sorted carbon nanotube networks. *Applied Physics Letters* 108 (10):103101. doi:10.1063/1.4942968.

Libich, J., J. Máca, J. Vondrák, O. Čech, and M. Sedlaříková. 2018. Supercapacitors: Properties and applications. *Journal of Energy Storage* 17:224–27. doi:10.1016/j.est.2018.03.012.

Liew, K. M., C. H. Wong, and M. J. Tan. 2006. Tensile and compressive properties of carbon nanotube bundles. *Acta Materialia* 54 (1):225–31. doi:10.1016/j.actamat.2005.09.002.

Likitchatchawankun, A., R. H. DeBlock, G. Whang, O. Munteshari, M. Frajnkovič, B. S. Dunn, and L. Pilon. 2021. Heat generation in electric double layer capacitors with neat and diluted ionic liquid electrolytes under large potential window between 5 and 80° C. *Journal of Power Sources* 488:229368. doi:10.1016/j.jpowsour.2020.229368.

Lim, H. -R., H. Seok Kim, R. Qazi, Y. -T. Kwon, J. -W. Jeong, and W. -H. Yeo. 2020. Advanced soft materials, sensor integrations, and applications of wearable flexible hybrid electronics in healthcare, energy, and environment. *Advanced Materials* 32 (15):1901924. doi:10.1002/adma.201901924.

Lin, C. -M., Y. -T. Lee, S. -R. Yeh, and W. Fang. 2009. Flexible carbon nanotubes electrode for neural recording. *Biosensors & Bioelectronics* 24 (9):2791–97. doi:10.1016/j.bios.2009.02.005.

Li, X., J. Shao, S. -K. Kim, C. Yao, J. Wang, Y. -R. Miao, Q. Zheng, P. Sun, R. Zhang, and P. V. Braun. 2018. High energy flexible supercapacitors formed via bottom-up infilling of gel electrolytes into thick porous electrodes. *Nature Communications* 9 (1):1–8. doi:10.1038/s41467-018-04937-8.

Liu, B., F. Wu, H. Gui, M. Zheng, and C. Zhou. 2017. Chirality-controlled synthesis and applications of single-wall carbon nanotubes. *ACS Nano* 11 (1):31–53. doi:10.1021/acsnano.6b06900.

Li, Y., K. Wang, J. Wei, Z. Gu, Z. Wang, J. Luo, and D. Wu. 2005. Tensile properties of long aligned double-walled carbon nanotube strands. *Carbon* 43 (1):31–35. doi:10.1016/j.carbon.2004.08.017.

Lota, K., V. Khomenko, and E. Frackowiak. 2004. Capacitance properties of poly (3, 4-ethylenedioxythiophene)/carbon nanotubes composites. *The Journal of Physics and Chemistry of Solids* 65 (2–3):295–301. doi:10.1016/j.jpcs.2003.10.051.

Lu, J. P. 1997. Elastic properties of carbon nanotubes and nanoropes. *Physical Review Letters* 79 (7):1297–300. doi:10.1103/PhysRevLett.79.1297.

Lu, X., and Z. Chen. 2005. Curved pi-conjugation, aromaticity, and the related chemistry of small fullerenes (< C60) and single-walled carbon nanotubes. *Chemical Reviews* 105 (10):3643–96. doi:10.1021/cr030093d.

Lukatskaya, M. R., B. Dunn, and Y. Gogotsi. 2016. Multidimensional materials and device architectures for future hybrid energy storage. *Nature Communications* 7 (1):1–13. doi:10.1038/ncomms12647.

Mahankali, K., N. Kumar Thangavel, Y. Ding, S. K. Putatunda, and L. Mohana Reddy Arava. 2019. Interfacial behavior of water-in-salt electrolytes at porous electrodes and its effect on supercapacitor performance. *Electrochimica acta* 326:134989. doi:10.1016/j.electacta.2019.134989.

Ma, Z., J. Zhao, Y. Fan, X. Qin, and G. Shao. 2022. High surface area of crystalline/amorphous ultrathin MnO2 nanosheets electrode for high-performance flexible micro-supercapacitors. *Journal of Alloys and Compounds* 920:166012. doi:10.1016/j.jallcom.2022.166012.

Mikhalchan, A., and J. José Vilatela. 2019. A perspective on high-performance CNT fibres for structural composites. *Carbon* 150:191–215. doi:10.1016/j.carbon.2019.04.113.

Mintmire, J. W., and C. T. White. 1995. Electronic and structural properties of carbon nanotubes. *Carbon* 33 (7):893–902. doi:10.1016/0008-6223(95)00018-9.

Mitra, M., and S. Gopalakrishnan. 2009. Wave propagation in multi-walled carbon nanotube. *Computational Materials Science* 45 (2):411–18. doi:10.1016/j.commatsci.2008.10.022.

Montazeri, A., J. Javadpour, A. Khavandi, A. Tcharkhtchi, and A. Mohajeri. 2010. Mechanical properties of multi-walled carbon nanotube/epoxy composites. *Materials & Design* 31 (9):4202–08. doi:10.1016/j.matdes.2010.04.018.

Moore, K. E., D. D. Tune, and B. S. Flavel. 2015. Double-walled carbon nanotube processing. *Advanced Materials* 27 (20):3105–37. doi:10.1002/adma.201405686.

Moradian, R., S. Azadi, and H. Refii-Tabar. 2007. When double-wall carbon nanotubes can become metallic or semiconducting. *Journal of Physics: Condensed Matter* 19 (17):176209. doi:10.1088/0953-8984/19/17/176209.

Muangrat, W., M. Obata, M. Than Htay, M. Fujishige, P. Dulyaseree, W. Wongwiriyapan, and Y. Hashimoto. 2021. Nitrogen-doped graphene nanosheet-double-walled carbon nanotube hybrid nanostructures for high-performance supercapacitors. *FlatChem* 29:100292. doi:10.1016/j.flatc.2021.100292.

Natsuki, T., T. Hayashi, and M. Endo. 2006. Mechanical properties of single-and double-walled carbon nanotubes under hydrostatic pressure. *Applied Physics A* 83 (1):13–17. doi:10.1007/s00339-005-3462-3.

Na, Y. W., J. Yeong Cheon, J. Ho Kim, Y. Jung, K. Lee, J. S. Park, J. Y. Park, K. Su Song, S. Bok Lee, T. Kim, et al. 2022. All-in-one flexible supercapacitor with ultrastable performance under extreme load. *Science Advances* 8 (1):eabl8631. doi:10.1126/sciadv.abl8631.

Nikita, G., S. Mital Gupta, and S. K. Sharma. 2019. Carbon nanotubes: Synthesis, properties and engineering applications. *Carbon Letters* 29 (5):419–47. doi:10.1007/s42823-019-00068-2.

Nurazzi, N. M., F. A. Sabaruddin, M. M. Harussani, S. H. Kamarudin, M. Rayung, M. R. M. Asyraf, H. A. Aisyah, M. N. F. Norrrahim, R. A. Ilyas, N. Abdullah, et al. 2021. Mechanical performance and applications of CNTs reinforced polymer composites—a review. *Nanomaterials (Basel)* 11 (9):2186. doi:10.3390/nano11092186.

Odom, T. W., J. -L. Huang, P. Kim, and C. M. Lieber. 2000. Structure and electronic properties of carbon nanotubes. *The Journal of Physical Chemistry B* 104 (13):2794–809. doi:10.1021/jp993592k.

Olabi, A. G., Q. Abbas, M. Ali Abdelkareem, A. Hai Alami, M. Mirzaeian, and E. Taha Sayed. 2023. Carbon-based materials for supercapacitors: recent progress, challenges and barriers. *Batteries* 9 (1):19. doi:10.3390/batteries9010019.

Park, S. J., S. T. Lim, M. S. Cho, H. M. Kim, J. Joo, and H. J. Choi. 2005. Electrical properties of multi-walled carbon nanotube/poly (methyl methacrylate) nanocomposite. *Current Applied Physics* 5 (4):302–04. doi:10.1016/j.cap.2004.02.013.

Park, S. K., Q. Mahmood, and H. Seok Park. 2013. Surface functional groups of carbon nanotubes to manipulate capacitive behaviors. *Nanoscale* 5 (24):12304–09. doi:10.1039/c3nr04858f.

Parvaneh, V., and M. Shariati. 2011. Effect of defects and loading on prediction of Young's modulus of SWCNTs. *Acta Mechanica* 216 (1):281–89. doi:10.1007/s00707-010-0373-y.

Patil, S. S., T. S. Bhat, A. M. Teli, S. A. Beknalkar, S. B. Dhavale, M. M. Faras, M. M. Karanjkar, and P. S. Patil. 2020. Hybrid solid state supercapacitors (Hssc's) for high energy & power density: An overview. *Engineered Science* 12 (4):38–51. doi:10.30919/es8d1140.

Peng, C., J. Jin, and G. Z. Chen. 2007. A comparative study on electrochemical co-deposition and capacitance of composite films of conducting polymers and carbon nanotubes. *Electrochimica acta* 53 (2):525–37. doi:10.1016/j.electacta.2007.07.004.

Pennington, G., and N. Goldsman. 2003. Semiclassical transport and phonon scattering of electrons in semiconducting carbon nanotubes. *Physical Review B* 68 (4):045426. doi:10.1103/PhysRevB.68.045426.

Popov, V. N. 2004. Carbon nanotubes: Properties and application. *Materials Science and Engineering: R: Reports* 43 (3):61–102. doi:10.1016/j.mser.2003.10.001.

Pu, S. -N., W. -Y. Yin, J. -F. Mao, and Q. H. Liu. 2009. Crosstalk prediction of single-and double-walled carbon-nanotube (SWCNT/DWCNT) bundle interconnects. *IEEE Transactions on Electron Devices* 56 (4):560–68. doi:10.1109/TED.2009.2014429.

Qian, Q., Y. Wang, M. Zhang, L. Chen, J. Feng, Y. Wang, and Y. Zhou. 2019. Ultrasensitive paper-based polyaniline/graphene composite strain sensor for sign language expression. *Compos Sci Tech* 181 (February):107660–107660. doi:10.1016/j.compscitech.2019.05.017.

Roche, S., F. Triozon, A. Rubio, and D. Mayou. 2001. Electronic conduction in multi-walled carbon nanotubes: Role of intershell coupling and incommensurability. *Physics Letters A* 285 (1–2):94–100. doi:10.1016/S0375-9601(01)00330-9.

Ryu, S., J. B. Chou, K. Lee, D. Lee, S. Hyung Hong, R. Zhao, H. Lee, and S. -G. Kim. 2015. Direct insulation-to-conduction transformation of adhesive catecholamine for simultaneous increases of electrical conductivity and mechanical strength of CNT fibers. *Advanced Materials* 27 (21):3250–55. doi:10.1002/adma.201500914.

Sadiq, M., M. Ajmal Khan, M. Moeen Hasan Raza, S. Masheerul Aalam, M. Zulfequar, and J. Ali. 2022. Enhancement of electrochemical stability window and electrical properties of CNT-Based PVA–PEG polymer blend composites. *ACS Omega* 7 (44):40116–31. doi:10.1021/acsomega.2c04933.

Salinas-Torres, D., R. Ruiz-Rosas, E. Morallón, and D. Cazorla-Amorós. 2019. Strategies to enhance the performance of electrochemical capacitors based on carbon materials. *Frontiers in Materials* 6. doi:10.3389/fmats.2019.00115.

Salvetat, J. P., J. M. Bonard, N. H. Thomson, A. J. Kulik, L. Forró, W. Benoit, and L. Zuppiroli. 1999. Mechanical properties of carbon nanotubes. *Applied Physics A* 69 (3):255–60. doi:10.1007/s003390050999.

Samy, M. M., M. G. Mohamed, A. F. M. El-Mahdy, T. Hassan Mansoure, K. C. W. Wu, and S. -W. Kuo. 2021. High-performance supercapacitor electrodes prepared from dispersions of tetrabenzonaphthalene-based conjugated microporous polymers and carbon nanotubes. *ACS Applied Materials & Interfaces* 13 (44):51906–16. doi:10.1021/acsami.1c05720.

Sandanayaka, A. S., N. K. Subbaiyan, S. K. Das, R. Chitta, E. Maligaspe, T. Hasobe, O. Ito, and F. D'Souza. 2011. Diameter-sorted SWCNT–Porphyrin and SWCNT–Phthalocyanine conjugates for light-energy harvesting. *ChemPhyschem* 12 (12):2266–73. doi:10.1002/cphc.201100377.

Shen, C., A. H. Brozena, and Y. Wang. 2011. Double-walled carbon nanotubes: Challenges and opportunities. *Nanoscale* 3 (2):503–18. doi:10.1039/C0NR00620C.

Shi, J., B. Jiang, Z. Liu, C. Li, F. Yan, X. Liu, H. Li, C. Yang, and D. Dong. 2021. Effects of specific surface area of electrode and different electrolyte on capacitance properties in nano porous-structure CrN thin film electrode for supercapacitor. *Ceramics International* 47 (13):18540–49. doi:10.1016/j.ceramint.2021.03.177.

Shin, D., H. Hwang, T. Yeo, S. Park, T. Kim, J. Lee, and W. Choi. 2019. Sol-gel-driven combustion wave for scalable transformation of Mn(NO3)2 precursors into MnO2-X/MWCNT supercapacitor electrodes capable of electrochemical activation. *Carbon* 152:746–54. doi:10.1016/j.carbon.2019.06.071.

Shiraishi, S., H. Kurihara, K. Okabe, D. Hulicova, and A. Oya. 2002. Electric double layer capacitance of highly pure single-walled carbon nanotubes (HiPco™ Buckytubes™) in propylene carbonate electrolytes. *Electrochemistry Communications* 4 (7):593–98. doi:10.1016/S1388-2481(02)00382-X.

Shi, S., C. Xu, C. Yang, J. Li, H. Du, B. Li, and F. Kang. 2013. Flexible supercapacitors. *Particuology* 11 (4):371–77. doi:10.1016/j.partic.2012.12.004.

Shokry, A., M. Karim, M. Khalil, S. Ebrahim, and J. El Nady. 2022. Supercapacitor based on polymeric binary composite of polythiophene and single-walled carbon nanotubes. *Scientific Reports* 12 (1):11278. doi:10.1038/s41598-022-15477-z.

Silki, S., A. Gupta, A. S. Maan, S. Dahiya, K. Singh, and A. Ohlan. 2022. Design and synthesis of polyaniline/MWCNT composite hydrogel as a binder-free flexible supercapacitor electrode. *Indian Journal of Physics* 96 (2):433–39. doi:10.1007/s12648-020-01996-w.

Sinha, P., and K. K. Kamal. 2020. Introduction to Supercapacitors. In *Handbook of nanocomposite supercapacitor materials II: Performance*, ed. K. K. Kar, 1–28. Cham: Springer International Publishing.

Soto, M., T. A. Boyer, S. Biradar, L. Ge, R. Vajtai, A. Elías-Zúñiga, P. M. Ajayan, and E. V. Barrera. 2015. Effect of interwall interaction on the electronic structure of double-walled carbon nanotubes. *Nanotechnology* 26 (16):165201. doi:10.1088/0957-4484/26/16/165201.

Stobinski, L., B. Lesiak, L. Kövér, J. Tóth, S. Biniak, G. Trykowski, and J. Judek. 2010. Multiwall carbon nanotubes purification and oxidation by nitric acid studied by the FTIR and electron spectroscopy methods. *Journal of Alloys and Compounds* 501 (1):77–84. doi:10.1016/j.jallcom.2010.04.032.

Strano, M. S., C. A. Dyke, M. L. Usrey, P. W. Barone, M. J. Allen, H. Shan, C. Kittrell, R. H. Hauge, J. M. Tour, and R. E. Smalley. 2003. Electronic structure control of single-walled carbon nanotube functionalization. *Science* 301 (5639):1519–22. doi:10.1126/science.1087901.

Sun, Y. -P., F. Kefu, Y. Lin, and W. Huang. 2002. Functionalized carbon nanotubes: Properties and applications. *Accounts of Chemical Research* 35 (12):1096–104. doi:10.1021/ar010160v.

Sun, Y., J. Sun, M. Liu, and Q. Chen. 2007. Mechanical strength of carbon nanotube–nickel nanocomposites. *Nanotechnology* 18 (50):505704. doi:10.1088/0957-4484/18/50/505704.

Swetha, C. 2022. Carbon nanotube electronics. In *Carbon nanotubes*, 209–34. Apple Academic Press.

Symeonidou, E.R., A. D. Nordin, W. David Hairston, and D. P. Ferris. 2018. Effects of cable sway, electrode surface area, and electrode mass on electroencephalography signal quality during motion. *Sensors* 18 (4):1073. doi:10.3390/s18041073.

Tange, M., T. Okazaki, and S. Iijima. 2011. Selective extraction of large-diameter single-wall carbon nanotubes with specific chiral indices by poly (9, 9-dioctylfluorene-alt-benzothiadiazole). *Journal of the American Chemical Society* 133 (31):11908–11. doi:10.1021/ja204698d.

Tian, Y., H. Du, M. Zhang, Y. Zheng, Q. Guo, H. Zhang, J. Luo, and X. Zhang. 2019. Microwave synthesis of MoS 2/MoO 2@ CNT nanocomposites with excellent cycling stability for supercapacitor electrodes. *Journal of Materials Chemistry C* 7 (31):9545–55. doi:10.1039/C9TC02391G.

Tounsi, A., S. Benguediab, A. Semmah, and M. Zidour. 2013. Nonlocal effects on thermal buckling properties of double-walled carbon nanotubes. *Advances in Nano Research* 1 (1):1. doi:10.12989/anr.2013.1.1.001.

Vangari, M., T. Pryor, and L. Jiang. 2013. Supercapacitors: Review of materials. *Journal of Energy Engineering (Ç)* 139 (2):72–79. doi:10.1061/(ASCE)EY.1943-7897.0000102.

Vashist, A., A. Kaushik, A. Vashist, V. Sagar, Y. G. Anujit Ghosal, S. Ahmad, and M. Nair. 2018. Advances in carbon nanotubes–hydrogel hybrids in nanomedicine for therapeutics. *Advanced Healthcare Materials* 7 (9):1701213. doi:10.1002/adhm.201701213.

Wang, H., Z. Cheng, Y. Liao, J. Li, J. Weber, A. Thomas, and C. F. J. Faul. 2017. Conjugated microporous polycarbazole networks as precursors for nitrogen-enriched microporous carbons for CO2 storage and electrochemical capacitors. *Chemistry of Materials* 29 (11):4885–93. doi:10.1021/acs.chemmater.7b00857.

Wang, Y., S. Gong, D. Dong, Y. Zhao, L. Wei Yap, Q. Shi, A. Tiance, Y. Ling, G. P. Simon, and W. Cheng. 2018. Self-assembled gold nanorime mesh conductors for invisible stretchable supercapacitors. *Nanoscale* 10 (34):15948–55. doi:10.1039/C8NR04256J.

Wang, D., C. Han, F. Mo, Q. Yang, Y. Zhao, Q. Li, G. Liang, B. Dong, and C. Zhi. 2020. Energy density issues of flexible energy storage devices. *Energy Storage Materials* 28:264–92. doi:10.1016/j.ensm.2020.03.006.

Wang, Y., X. Wu, Y. Han, and T. Li. 2021. Flexible supercapacitor: Overview and outlooks. *Journal of Energy Storage* 42:103053. doi:10.1016/j.est.2021.103053.

Wang, B., H. Xin, X. Li, J. Cheng, G. Yang, and F. Nie. 2014. Mesoporous CNT@ TiO2-C nanocable with extremely durable high rate capability for lithium-ion battery anodes. *Scientific Reports* 4 (1):1–7. doi:10.1038/srep03729.

Wang, Z., M. Zhu, Z. Pei, Q. Xue, L. Hongfei, Y. Huang, and C. Zhi. 2020. Polymers for supercapacitors: Boosting the development of the flexible and wearable energy storage. *Materials Science and Engineering: R: Reports* 139:100520. doi:10.1016/j.mser.2019.100520.

Wavhal, B. A., M. Ghosh, S. Sharma, S. Kurungot, and S. Asha. 2021. A high-voltage non-aqueous hybrid supercapacitor based on the N2200 polymer supported over multiwalled carbon nanotubes. *Nanoscale* 13 (28):12314–26. doi:10.1039/D1NR01422F.

Weber, J., and A. Thomas. 2008. Toward stable interfaces in conjugated polymers: Microporous Poly(p-phenylene) and Poly(phenyleneethynylene) based on a spirobifluorene building block. *Journal of the American Chemical Society* 130 (20):6334–35. doi:10.1021/ja801691x.

Wei, J., H. Zhu, B. Jiang, L. Ci, and D. Wu. 2003. Electronic properties of double-walled carbon nanotube films. *Carbon* 41 (13):2495–500. doi:10.1016/S0008-6223(03)00295-1.

WenXing, B., Z. ChangChun, and C. WanZhao. 2004. Simulation of Young's modulus of single-walled carbon nanotubes by molecular dynamics. *Physica B, Condensed Matter* 352 (1–4):156–63. doi:10.1016/j.physb.2004.07.005.

Wimalasiri, Y., and L. Zou. 2013. Carbon nanotube/graphene composite for enhanced capacitive deionization performance. *Carbon* 59:464–71. doi:10.1016/j.carbon.2013.03.040.

Wu, L., Y. Han, Q. Zhao, and L. Zhang. 2021. Effects of chiral indices on the atomic arrangements and electronic properties of Si double-walled nanotubes (6, min)@(9, mout)(min= 0 to 6, mout= 0 to 9) by SCC-DFTB calculations. *Materials Science in Semiconductor Processing* 129:105775. doi:10.1016/j.mssp.2021.105775.

Xia, Y., M. Yoshio, and H. Noguchi. 2006. Improved electrochemical performance of LiFePO4 by increasing its specific surface area. *Electrochimica acta* 52 (1):240–45. doi:10.1016/j.electacta.2006.05.002.

Xie, J., P. Yang, Y. Wang, T. Qi, Y. Lei, and C. M. Li. 2018. Puzzles and confusions in supercapacitor and battery: Theory and solutions. *Journal of Power Sources* 401:213–23. doi:10.1016/j.jpowsour.2018.08.090.

Xu, R., A. Zverev, A. Hung, C. Shen, L. Irie, G. Ding, M. Whitmeyer, L. Ren, B. Griffin, J. Melcher, et al. 2018. Kirigami-inspired, highly stretchable micro-supercapacitor patches fabricated by laser conversion and cutting. *Microsystems & Nanoengineering* 4 (1):1–10. doi:10.1038/s41378-018-0036-z.

Yang, H. 2020. A comparative study of supercapacitor capacitance characterization methods. *Journal of Energy Storage* 29:101316. doi:10.1016/j.est.2020.101316.

Yang, D., D. Tian, C. Xue, F. Gao, Y. Liu, H. Li, Y. Bao, J. Liang, Z. Zhao, and J. Qiu. 2018. Tuned fabrication of the aligned and opened CNT membrane with exceptionally high permeability and selectivity for bioalcohol recovery. *Nano Letters* 18 (10):6150–56. doi:10.1021/acs.nanolett.8b01831.

Yeh, M. -K., T. -H. Hsieh, and N. -H. Tai. 2008. Fabrication and mechanical properties of multi-walled carbon nanotubes/epoxy nanocomposites. *Materials Science and Engineering A* 483-484:289–92. doi:10.1016/j.msea.2006.09.138.

Yu, Z., L. Tetard, L. Zhai, and J. Thomas. 2015. Supercapacitor electrode materials: Nanostructures from 0 to 3 dimensions. *Energy & Environmental Science* 8 (3):702–30. doi:10.1039/C4EE03229B.

Zaheer, M. M., M. Shamsuddin Jafri, and R. Sharma. 2019. Effect of diameter of MWCNT reinforcements on the mechanical properties of cement composites. *Advanced Concrete Construction* 8 (3):207–15.

Zaporotskova, I. V., N. P. Boroznina, Y. N. Parkhomenko, and L. V. Kozhitov. 2016. Carbon nanotubes: Sensor properties. A review. *Modern Electronic Materials* 2 (4):95–105. doi:10.1016/j.moem.2017.02.002.

Zhang, L., R. Jamal, Q. Zhao, M. Wang, and T. Abdiryim. 2015. Preparation of PEDOT/GO, PEDOT/MnO2, and PEDOT/GO/MnO2 nanocomposites and their application in catalytic degradation of methylene blue. *Nanoscale Research Letters* 10 (1):148. doi:10.1186/s11671-015-0859-6.

Zhang, C. -L., and H. -S. Shen. 2008. Predicting the elastic properties of double-walled carbon nanotubes by molecular dynamics simulation. *Journal of Physics D: Applied Physics* 41 (5):055404. doi:10.1088/0022-3727/41/5/055404.

Zhang, Y. Y., V. B. C. Tan, and C. M. Wang. 2007. Effect of strain rate on the buckling behavior of single-and double-walled carbon nanotubes. *Carbon* 45 (3):514–23. doi:10.1016/j.carbon.2006.10.020.

Zhang, T., Z. S. Yuan, and L. H. Tan. 2011. Exact geometric relationships, symmetry breaking and structural stability for single-walled carbon nanotubes. *Nano-Micro Letters* 3 (4):228–35. doi:10.1007/BF03353677.

Zhang, Y., H. Zhang, F. Jiang, W. Zhou, R. Wang, J. Xu, X. Duan, Y. Wu, and Y. Ding. 2020. Electrochemical assembly of homogenized poly(3,4-ethylenedioxythiophene methanol)/SWCNT nano-networks and their high performances for supercapacitor electrodes. *Ionics* 26 (7):3631–42. doi:10.1007/s11581-020-03475-y.

Zhao, Q., G. Wang, K. Yan, J. Yan, and J. Wang. 2015. Binder-free porous PEDOT electrodes for flexible supercapacitors. *Journal of Applied Polymer Science* 132 (41). doi:10.1002/app.42549.

Zhou, M., Y. Li, Q. Gong, Z. Xia, Y. Yang, X. Liu, J. Wang, and Q. Gao. 2019. Polythiophene grafted onto single-wall carbon nanotubes through Oligo(ethylene oxide) linkages for supercapacitor devices with enhanced electrochemical performance. *ChemElectrochem* 6 (17):4595–607. doi:10.1002/celc.201901074.

Zhou, Z., M. Steigerwald, M. Hybertsen, L. Brus, and R. A. Friesner. 2004. Electronic structure of tubular aromatic molecules derived from the metallic (5, 5) armchair single wall carbon nanotube. *Journal of the American Chemical Society* 126 (11):3597–607. doi:10.1021/ja039294p.

Zólyomi, V., Á. Rusznyák, J. Kürti, Á. Gali, F. Simon, H. Kuzmany, Á. Szabados, and P. R. Surján. 2006. Semiconductor-to-metal transition of double walled carbon nanotubes induced by inter-shell interaction. *Physica Status Solidi (B)* 243 (13):3476–79. doi:10.1002/pssb.200669161.